AD

Research and Development Technical Report
ECOM-3574

FERRITE ROD ANTENNA ARRAYS FOR LORAN-C RECEIVERS

Kurt Ikrath

May 1972

Details of illustrations in this document may be better studied on microfiche

DISTRIBUTION STATEMENT

Approved for public release; distribution unlimited.

ECOM

UNITED STATES ARMY ELECTRONICS COMMAND · FORT MONMOUTH, N.J.

74

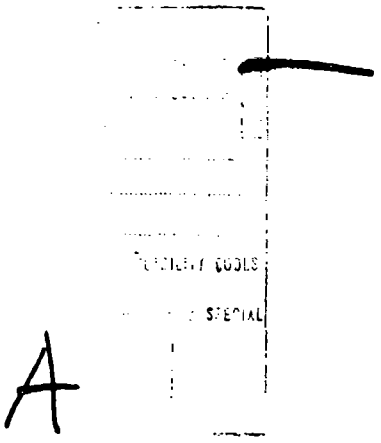

NOTICES

Disclaimers

The findings in this report are not to be construed as an official Department of the Army position, unless so designated by other authorized documents.

The citation of trade names and names of manufacturers in this report is not to be construed as official Government indorsement or approval of commercial products or services referenced herein.

Disposition

Destroy this report when it is no longer needed. Do not return it to the originator.

UNCLASSIFIED

Security Classification

DOCUMENT CONTROL DATA - R & D

(Security classification of title, body of abstract and indexing annotation must be entered when the overall report is classified)

1. ORIGINATING ACTIVITY (Corporate author)
U.S. Army Electronics Command
Fort Monmouth, New Jersey 07703

2a. REPORT SECURITY CLASSIFICATION
UNCLASSIFIED

2b. GROUP

3. REPORT TITLE

Ferrite Rod Antenna Arrays for Loran-C Receivers

4. DESCRIPTIVE NOTES (Type of report and inclusive dates)
Technical Report

5. AUTHOR(S) (First name, middle initial, last name)

Kurt Ikrath

6. REPORT DATE	7a. TOTAL NO. OF PAGES	7b. NO. OF REFS
May 1972	66	4

8a. CONTRACT OR GRANT NO.	9a. ORIGINATOR'S REPORT NUMBER(S)
b. PROJECT NO. 1H6 62701 A448	ECOM-3574
c. Task No. -06	9b. OTHER REPORT NO(S) (Any other numbers that may be assigned this report)
d. Work Unit No. -221	

10. DISTRIBUTION STATEMENT

Approved for public release; distribution unlimited.

11. SUPPLEMENTARY NOTES	12. SPONSORING MILITARY ACTIVITY
	U. S. Army Electronics Command ATTN: AMSEL-NL-R-4 Fort Monmouth, N.J. 07703

13. ABSTRACT

The use of a small ferrite antenna array is shown theoretically to be superior in performance to the whip antenna supplied with a PSN-4 Loran-C receiver manpack set. While the paper is overall theoretical in nature, the theoretical results and conclusions have been verified in subsequent limited experimentation.

Initial test with a compact ferrite rod antenna array in place of a whip showed that the time for acquisition of Loran-C time coordinates with the PSN-4 set is reduced to about one third the time it takes with a 15 foot long whip.

DD FORM 1 NOV 68 1473 REPLACES DD FORM 1473, 1 JAN 64, WHICH IS OBSOLETE FOR ARMY USE.

UNCLASSIFIED

Security Classification

14. KEY WORDS	LINK A		LINK B		LINK C	
	ROLE	WT	ROLE	WT	ROLE	WT
Ferrite Rod						
Antenna Arrays						

HISA-FM-1801-72

Reports Control Symbol OSD-1366

TECHNICAL REPORT ECOM- 3574

FERRITE ROD ANTENNA ARRAYS FOR LORAN-C RECEIVERS

by

Kurt Ikrath

Communications/Automatic Processing Laboratory

DA Work Unit #1H6 62701 A448 06 22 1

JUNE 1972

US ARMY ELECTRONICS COMMAND

FORT MONMOUTH, NEW JERSEY 07703

ABSTRACT

The use of a small ferrite antenna array is shown theoretically to be superior in performance to the whip antenna supplied with a PSN-4 Loran-C receiver manpack set. While the paper is basically theoretical in nature, the theoretical results and conclusions have been verified in subsequent limited experimentation.

Initial test with a compact ferrite rod antenna array in place of a whip showed that the time for acquisition of Loran-C time coordinates with the PSN-4 set is reduced to about one third the time it takes with a 15 foot long whip.

TABLE OF CONTENTS

LIST OF FIGURES

Introduction

Loran-C Long Range Navigation Systems employ a 100 kHz radio carrier frequency; by comparison with standard Loran which operates on a carrier frequency of 1850 kHz, 1900 kHz, or 1950 kHz, Loran-C provides a longer ground wave range. All ground wave radio navigation systems are sensitive to ground and terrain induced propagation effects, including seasonal variations of ground conductivities due to vegetation, rain, snow and frost; propagation - ground effects cause inaccuracies in the determination of a receiver's actual geographic position from the time difference of pulse signals which he receives from distant Loran master and slave transmitters. Locally, ground effects manifest themselves in the electrical fields' polarization which ranges from almost vertical over seawater to forward in the direction of propagation tilted, linear and elliptical polarization over land; in the latter case, the electrical field strength becomes also a minimum at fractions of a wavelength high above ground. In particular, mountains and boundaries between different earth and water media and corresponding discontinuities of electrical surface impedances affect directly the polarization and phase of the electrical field relative to the horizontally polarized magnetic field. The lower sensitivity to ground effects of the long wave Loran-C System relative to the medium wave standard Loran System is offset to some extent by the need of physically larger antennas and by the higher noise levels in the lower part of the radio spectrum; in particular, by quasi-static type tribo electric and atmospheric noise and by man-made radio frequency interference (RFI).

One may call this local noise time-like in contrast to the parametric type perturbation of the signal amplitude and phase by ground effects which constitutes space-like noise. Since short whip antennas, i.e., quasi-static electrical antennas, as they are used with Loran-C receiver manpack sets (PSN-4) are highly susceptible to both space-like noise (ground effects) and time-like noise (spherics and RFI), whip antennas are a severe handicap for the operation of Loran-C manpack receivers under field conditions. Under these conditions, it becomes more advantageous to use magnetic antennas in the form of ferrite rod arrays which are described in the subsequent discussion.

Discussion

1. Effective Height, Magnetization, and Relative Effective Magnetic Permeability of Ferrite Rod Antennas

The effective height h_w of a short whip antenna with a height H of 2 to 6 meters at long and medium wave radio frequencies is given approximately by

$$h_w \doteq \frac{2}{\pi} \cdot H \qquad (1)$$

In practice, this effective height is numerically about 100 to 1000 times larger than the effective height of a typical 10 to 20 cm long ferrite antenna rod; the effective height h_f of a ferrite antenna is given by

$$h_F \doteq \frac{2\pi w \cdot q}{\lambda} \cdot \mu_{eff.rel.} \qquad (2)$$

where w is the number of turns of the wire windings, q the crossection area of the rod, $\mu_{eff.rel.}$ its effective relative permeability and λ the wavelength.

However, aperiodic whip antennas lack the high Q and the directivity which enable small compact ferrite rod antennas to compete successfully with the larger whips in the medium and the long wave frequency range.[1] The Q corrected effective height h_f' of a ferrite rod antenna which forms the inductance part of a parallel tuned resonant circuit is given by

$$h_F' = Q \cdot h_F \qquad (3)$$

The effective permeability is defined theoretically by

$$\mu_{eff} = \frac{B^{(i)}}{H^{(p)}} \qquad (4)$$

$H^{(p)}$ is here the primary homogeneous magnetic excitation field in Amp-meter^{-1} and $B^{(i)}$ the flux density in Volts-seconds-meter^{-2} (i.e., teslas) inside an ellipsoid shaped body of magnetic material, such that the major axis of the ellipsoid is aligned with the direction of primary field $H^{(p)}$. This elliptic geometry produces also a homogeneous type magnetic polarization P_m, i.e., a magnetization which is a function of the internal magnetic field $H^{(i)}$. The magnetization is given numerically as the flux density which is contributed by the magnetic properties of the material and expressed by P_m in the following equation:

$$B^{(i)} = \mu_0 H^{(i)} + P_m \qquad (5)$$

where $\mu_0 = 0.4\pi \times 10^{-6}$ in Volt seconds over ampere x meter is the permeability of free space in the rationalized MKS system. The magnetic susceptibility χ of the material relates the magnetization P_m and the internal field in the form of a linear relation.

$$P_m = \chi \mu_0 H^{(i)} \tag{6}$$

The intrinsic magnetic permeability of the material can then be expressed as

$$\mu_i = \frac{B^{(i)}}{H^{(i)}} = \mu_0 (1+\chi) \tag{7}$$

This is the permeability which one measures with toroidal core-shaped, magnetic solenoids where $H^{(p)}$ and $H^{(i)}$ are identical. In the ellipsoid case, the internal field $H^{(i)}$ is derived as function of the primary excitation field $H^{(p)}$ from the dimensions and the magnetic susceptibility χ of the material with

$$H^{(i)} = \frac{H^{(p)}}{1+\chi \cdot \left[\left(\frac{b}{c}\right)^2 \cdot \left[\frac{a}{2c} \cdot \ln \frac{a/c+1}{a/c-1} - 1\right]\right]} \tag{8}$$

Here are 2a and 2b, the major and minor axes of an ellipsoid, and $2c = 2\sqrt{a^2-b^2}$, the distance between the focal points. The formula in Equation (8) is given in the literature;[2,3] however, for completeness of the subsequently discussed interaction between ferrite rods in array configurations, this formula is derived in Appendix A.

Using Equations (4) to (6), in conjunction with Equation (8), one obtains the effective relative permeability in the familiar form

$$\mu_{eff.rel} = \frac{\mu_{i\,rel}}{1 - (\mu_{i\,rel}-1) \cdot N} \tag{9}$$

The factor N in the denominator is given by

$$N = \left[\left(\frac{b}{c}\right)^2 \cdot \left[\frac{a}{2c} \cdot \ln \frac{a/c + 1}{a/c - 1} - 1\right]\right] \qquad (10)$$

and is called the form factor or demagnetization factor.

In practice where cylindrical rods of length l and diameter d are used, the magnetization is not homogeneous and the corresponding effective relative permeability cannot be derived theoretically. In this case, the following empirically determined form factor is used.[4]

$$N = (0.84) \cdot \left(\frac{d}{l}\right)^{1.7} \qquad (11)$$

The graph in Fig. 1 shows that the theoretical and the empirical values of $\mu_{eff.rel.}$ for the ellipsoid and the cylinder tend to conform for length to diameter ratios which exceed five to one.

For the design of ferrite rod antenna arrays, one needs the magnetization and the associated secondary type external field rather than the effective permeabilities; considering two types of array configurations, longitudinal and transverse arrays, one must know the external secondary field at the locations which are denoted in Figure 2 by Roman one and two; the values of the secondary fields, H_I and H_{II} at these locations, at distances z and ρ, respectively, from the center of the magnetic ellipsoid, are derived in Appendix A.

These fields may be expressed as secondary dipole fields:

$$H_I^{(s)} = \frac{m_z}{2\pi \cdot \mu_0 |z|^3} \qquad (12)$$

$$H_{II}^{(s)} = \frac{m_z}{2\pi \mu_0 |\rho|^3} \qquad (13)$$

where M_z, the secondary magnetic dipole-moment, is given by the volume integral over the magnetization. In our case, the integral reduces to the product of volume and magnetization by the primary field:

$$M_z = \{Vol.\} \cdot \{P_m\} = \frac{4\pi}{3} b^2 a \cdot \frac{\chi}{1+\chi N} \cdot \mu_0 H^{(p)} \qquad (14)$$

Magnetization, corresponding dipole moments and associated secondary type external fields are explored further in the following section which is entitled, Longitudinal "Type Ferrite Rod Antenna Arrays."

2. Longitudinal Type Ferrite Rod Antenna Arrays

The principles that govern the mutual magnetic coupling and the relevant mathematics are introduced, by considering the insertion of a second identical magnetic ellipsoid into the field that results from the superposition of the original primary field and of the secondary field of the first ellipsoid.

Referring to the sketch in Figure 3, one recognizes that first, the second ellipsoid will be magnetized by this field, which we denote as the first resultant field. The magnetization of the second ellipsoid by the first resultant field produces again a secondary field that creates an additional magnetization in the first ellipsoid; this additional magnetization of the first ellipsoid, produces an additional secondary field, which when superimposed over the first resultant field forms the second resultant field. This field produces an additional magnetization in the second ellipsoid and a corresponding additional secondary field which when superimposed over the second resultant field forms the third resultant field. The third resultant field produces an additional magnetization in the first ellipsoid and so on. Evidently, the mutual coupling leads to the generation of a convergent series of magnetization terms, the sum of which yields the final actual magnetization of each ellipsoid.

It is evident, from the dipole character of the secondary fields, that the magnetization associated with the mutual coupling between the ellipsoids will be inhomogeneous. However, when the distance h between the center of the first and of the second ellipsoid satisfies the inequality

$$h \gg \sqrt[3]{\frac{2b^2 a}{3} \cdot \frac{\chi}{1+\chi N}} \qquad (15)$$

the homogeneous magnetization approach is valid. This approach which is described in detail in Appendix B, yields a geometric progression for the final magnetization of each ellipsoid and a resultant effective relative permeability:

$$\mu_{eff.rel.} \doteq \frac{\chi+1}{1+\chi N} \cdot \frac{1}{\left[1-\frac{2b^2a}{3lh^3}\cdot\frac{\chi}{1+\chi N}\right]} \qquad (16)$$

Here $\chi=\mu_{i.rel}-1$ the intrinsic magnetic susceptibility of the material and N the form factor of the identical ellipsoids.

In accordance with the previously discussed approximation of cylindrical rods by long ellipsoids, the result is also applicable to cylindrical rods.

Using the same mathematical procedure, the magnetization of each ellipsoid, or similar rod element in a three element longitudinal array, is derived in Appendix C. The resultant effective relative permeabilities are given as follows:

For the end elements:

$$\left(\mu_{eff.rel}\right)_{end} = \frac{1+\chi}{1+\chi N} \cdot \frac{1+\left(\frac{2b^2a}{3lh^3}\right)\cdot\left(\frac{\chi}{1+\chi N}\right)}{1-2\cdot\left[\left(\frac{2b^2a}{3lh^3}\right)\cdot\left(\frac{\chi}{1+\chi N}\right)\right]^2} \qquad (17)$$

For the center element:

$$\left(\mu_{eff.rel}\right)_{center} = \frac{1+\chi}{1+\chi N} \cdot \frac{1+2\left(\frac{2b^2a}{3lh^3}\right)\left(\frac{\chi}{1+\chi N}\right)}{1-2\left[\left(\frac{2b^2a}{3lh^3}\right)\left(\frac{\chi}{1+\chi N}\right)\right]^2} \qquad (18)$$

The higher degree of magnetization of the center element due to the secondary fields from both the left hand and the right hand end element (Fig. 4) is reflected by the factor 2 in the numerator term in Equation (18). In general, mutual coupling between longitudinal aligned elements in a ferrite rod antenna array increases the relative effective permeability relative to that of a single rod; the subsequent numerical examples provide a quantitative insight into mutual coupling effects.

3. Numerical Examples

The orders of magnitude of the increases in the effective relative permeability, due to mutual coupling between ferrite rod antenna elements

in longitudinal arrays, are given in detail in Appendix D. For the purpose of the following discussion, assume an intrinsic permeability value

$$\mu_{i\,rel} = \chi + 1 = 200 \tag{19}$$

and apply the theoretical ellipsoid approach to a cylindrical rod with a length 2a = 16 cm and a diameter 2b = 2 cm, i.e., $\frac{a}{b} = 8$.

The form factor is in this case $N = 0.0275$.

Equation (9) for the single rod (ellipsoid) becomes then

$$\mu_{eff.rel} \doteq \frac{200}{1 + (199) \cdot [0.0275]} \doteq 30 \tag{20}$$

Using this value in Equations (16), (17), and (18) for the two and three element array, it becomes convenient for the further numerical calculations to introduce the separation h between elements normalized with respect to rod length in the following form:

$$h = k \cdot 2a \tag{21}$$

where k will be referred to as separation parameter. As a consequence of the introduction of the separation parameter k into the equations for the effective relative permeabilities of array elements, one needs the expression:

$$\frac{2b^2 a}{3|h|^3} = \frac{1}{12}\left(\frac{b}{a}\right)^2 \cdot \frac{1}{k^3} \tag{22}$$

Introducing the chosen numerical values (a/b = 8, $\mu_{eff.rel} = 30$) and the corresponding values of Equation (22), ($0.0013/k^3$) into Equation (16), one gets the effective relative permeability of each element in the two element array:

$$\mu_{eff.rel} \doteq \frac{30}{1 - \frac{0.0013}{k^3} \cdot 30} \tag{23}$$

Values for different k and corresponding separation

$$\Delta = 2a(k-1) \tag{24}$$

between the adjacent ends of the elements in the two element array are tabulated below:

k	Δ/cm	$\mu_{\text{eff rel.}}$
1.13	2.08	30 (1 + 0.03)
1.48	7.8	30 (1 + 0.015)
1.93	14.9	30 (1 + 0.006)

Similarly, for the three element array, follow from Equations (17) and (18), the effective relative permeabilities for the end elements with

$$(\mu_{\text{eff. rel}})_{\text{end}} \doteq 30 \cdot \frac{1 + \left(\frac{0.0013}{k^3}\right)\cdot(30)}{1 - 2\left[\left(\frac{0.0013}{k^3}\right)(30)\right]^2} \tag{25}$$

and for the center element with

$$(\mu_{\text{eff. rel}})_{\text{center}} \doteq 30 \cdot \frac{1 + 2\cdot\left(\frac{0.0013}{k^3}\right)\cdot(30)}{1 - 2\left[\left(\frac{0.0013}{k^3}\right)(30)\right]^2} \tag{26}$$

Typical numerical values of these effective relative permeabilities are tabulated below.

k	Δ/cm	(μ eff rel) end	($\mu_{\text{eff rel.}}$) center
1.13	2.08	30 (1 + 0.03180)	30 (1 + 0.0618)
1.48	7.8	30 (1 + 0.01545)	30 (1 + 0.0345)
1.93	14.9	30 (1 + 0.006)	30 (1 + 0.012

These numerical results indicate that in practice the mutual magnetic coupling between ferrite rod antenna elements in a longitudinal array increases the effective permeabilities of each element by a few percent. Consequently, when one extends the calculations to longitudinal arrays with more then three ferrite rod elements, a sufficient degree of accuracy is obtained from the initial terms in the series expansions for the magnetizations. For example, the effective relative permeabilities of the end 1 , intermediate 2 , and center 3 elements in a 6 element longitudinal ferrite rod antenna array, are approximated in this case by:

$$(\mu_{eff.rel})_1 \doteq \frac{(1+\chi)}{1+\chi N}\left[1+\frac{\chi}{1+\chi N}\cdot\frac{(b/a)^2}{12k^3}\left[\frac{1}{1^3}+\frac{1}{2^3}+\frac{1}{3^3}+\cdots\right]\right] \quad (27)$$

$$(\mu_{eff\,rel})_2 \doteq \frac{(1+\chi)}{1+\chi N}\left[1+\frac{\chi}{1+\chi N}\cdot\frac{(b/a)^2}{12k^3}\left[\frac{2}{1^3}+\frac{1}{2^3}+\frac{1}{3^3}+\cdots\right]\right] \quad (28)$$

$$(\mu_{eff\,rel})_3 \doteq \frac{(1+\chi)}{1+\chi N}\left[1+\frac{\chi}{1+\chi N}\cdot\frac{(b/a)^2}{12k^3}\left[\frac{2}{1^3}+\frac{2}{2^3}+\frac{1}{3^3}+\cdots\right]\right] \quad (29)$$

Similarly, as in longitudinal arrays, mutual coupling between ferrite rod antenna elements in transverse arrays contributes to the effective permeability of each element. However, as seen in the following section, mutual coupling between elements in transverse arrays is in effect a mutual shielding that lowers the effective permeability of each element.

4. Transverse Type Ferrite Rod Antenna Arrays

In the transverse array case, the secondary fields involve instead of H_I of Equation (12) the opposite H_{II} of Equation (13). As a consequence of the iterative superposition of primary and secondary fields, the resultant magnetizations are, in this case, decreased. The corresponding lowered effective relative permeabilities for each ferrite rod antenna element in two and three element transverse arrays are derived in Appendices E to G.

For a two element array, such as sketched in Fig. 5, one arrives at different approximations for the effective relative permeabilities dependent on the range of separation h' between the array elements. Introducing for this purpose the separation parameter k' defined in terms of the diameter 2b of the equivalent ellipsoid, one obtains the following approximations:

$$\mu_{eff\,rel} \doteq \frac{1+\chi}{1+\chi N} \cdot \begin{cases} \left[\dfrac{1}{1+\dfrac{a/b}{24\cdot k'^3}\cdot\dfrac{\chi}{1+\chi N}}\right] & \text{for } k'=\dfrac{h'}{2b} \gg \dfrac{a}{2b} \\ \left[\dfrac{1}{1+\dfrac{(b/a)^2\chi}{1+\chi N}\cdot\dfrac{1}{3\left[1+(b/a)^2(2k')^2\right]^{3/2}}}\right] & \text{for } 1<k'\leq\dfrac{a}{2b} \end{cases}$$

Similarly, for three element transverse arrays, the effective relative permeabilities for the center element are given by

$$\left(\mu_{eff\,rel}\right)_{center} \doteq \frac{1+\chi}{1+\chi N} \cdot \begin{cases} \left[\dfrac{1-2\,\dfrac{a/b}{24}\cdot\dfrac{\chi}{1+\chi N}\cdot\dfrac{1}{|k'|^3}}{1-2\left[\dfrac{a/b}{24}\cdot\dfrac{\chi}{1+\chi N}\cdot\dfrac{1}{|k'|^3}\right]^2}\right] & \text{for } k' \gg \dfrac{a}{2b} \\ \left[\dfrac{1-2\,\dfrac{\chi(b/a)^2}{1+\chi N}\cdot\dfrac{1}{3\left[1+(b/a)^2(2k')^2\right]^{3/2}}}{1-2\left[\dfrac{\chi(b/a)^2}{1+\chi N}\cdot\dfrac{1}{3\left[1+(b/a)^2(2k')^2\right]^{3/2}}\right]^2}\right] & \text{for } 1<k'\leq\dfrac{a}{2b} \end{cases}$$

and for the end elements by

$$\left(\mu_{eff.rel}\right)_{end} \doteq \frac{1+\chi}{1+\chi N} \cdot \begin{cases} \left[\dfrac{1-\frac{a/b}{24}\cdot\dfrac{\chi}{1+\chi N}\cdot\dfrac{1}{|k'|^3}}{1-2\left[\frac{a/b}{24}\cdot\dfrac{\chi}{1+\chi N}\cdot\dfrac{1}{|k'|^3}\right]^2}\right]_{\text{for } k' \geq \frac{a}{2b}} \\ \left[\dfrac{1-\dfrac{\chi\left(\frac{b}{a}\right)^2}{1+\chi N}\cdot\dfrac{1}{3\left[1+(b/a)^2(2k')^2\right]^{3/2}}}{1-2\left[\dfrac{\chi\left(\frac{b}{a}\right)^2}{1+\chi N}\cdot\dfrac{1}{3\cdot\left[1+(b/a)^2(2k')^2\right]^{3/2}}\right]}\right]_{\text{for } 1<k'\leq\frac{a}{2b}} \end{cases}$$

Introducing into these formulas the previously used numerical values $\chi = 199$, $\frac{a}{b} = 8$ and $N = 0.0275$, one obtains the subsequently tabulated numerical values for the effective relative permeabilities as functions of separations in two and three element transverse arrays.

For the Two Element Transverse Array

$k' = \frac{h'}{2b}$	$\mu_{rel.\,eff}$
1	30 (1 - 0.142)
1.5	30 (1 - 0.13)
2.0	30 (1 - 0.112)
3.0	30 (1-0.080)
4.0	30 (1 - 0.056)
6.0	30 (1 - 0.026)
8.0	30 (1 - 0.014)
10.0	30 (1 - 0.008)
20.0	30 (1 - 0.00125)
	30

For the Three Element Transverse Array

$k' = \frac{h'}{2b}$	End Rod μ rel eff	Center Rod μ rel eff
1	30 (1 - 0.14)	30 (1 - 0.28)
1.5	30 (1 - 0.13)	30 (1 - 0.26)
2.0	30 (1 - 0.11)	30 (1 - 0.22)
2.5	30 (1 - 0.096)	30 (1 - 0.192)
3.0	30 (1 - 0.08)	30 (1 - 0.16)
4.0	30 (1 - 0.056)	30 (1 - 0.11)
6.0	30 (1 - 0.0266)	30 (1 - 0.052)
8.0	30 (1 - 0.014)	30 (1 - 0.028)
10.0	30 (1 - 0.008)	30 (1 - 0.016)
20.0	30 (1 - 0.00125)	30 (1 - 0.0025)

5. Experimental Implementations

Commercially available rods of type H Ferramic material* were used for the construction of various ferrite rod antenna arrays. A typical ferrite rod antenna element from which these arrays were constructed is shown in Fig. 6. The electrical winding on this rod has 380 turns which are divided equally into left and right handed wound sections to reduce the capacitive effects. The windings are insulated from the ferrite rod surface by a thin layer of mylar insulation. Six of these rod elements are used in the transverse ferrite rod antenna array shown in Fig. 7 connected to the PSN-4 Loran-C receiver set at a location near a building in the Evans, N.J. area. Figure 8 shows a close-up view of the PSN-4 digital output device which displays the Loran-C time coordinates of this receiver location.

Loran-C signal receptions are improved further with the twin array seen in Figure 9 mounted on a weapons carrier.

This twin array consists of a pair of 7 element transverse array packages which can be rotated relative to each other for optimum simultaneous reception of Loran-C master and slave station signals which arrive from different directions at the receiver locations.

*Trade Name for ferrite material manufactured by Indiana General Co.

Conclusions

Initial Loran-C signal reception tests, using the compact ferrite rod antenna arrays instead of the standard whip antenna, showed that the time for acquisition of Loran-C time coordinates with the PSN-4 set is reduced to about one third the time it takes with the 15 foot long whip mounted on the roof of Building T-113 in the Evans area. The reductions of the coordinate acquisition times were measured early in the morning when atmospheric and man-made noise interference levels are relatively low. During the day and towards evenings, the noise levels increase and propagation conditions change; therefore, the whip antenna was then unable to deliver the pulse signals from the most distant Slave B station located at Dana, Indiana* to the PSN-4 set, whereas, using the ferrite arrays the PSN-4 set locked to the B slave and the corresponding coordinates were displayed within two to three minutes after turning the set on.

Acknowledgments

The improvement of Loran-C navigation by means of compact magnetic tape ferrite rod antenna arrays is a cooperative effort of personnel from ECOM's Comm/ADP, Avionics, and Electronics Technology & Devices Laboratories.

Special thanks go to Mr. Granville Le Meune who constructed the experimental ferrite rod antenna arrays.

*Master and Slave A stations are at Cape Fear, North Carolina, and Nantucket, Massachusetts, respectively.

References

1. Snelling, E. C., "Ferrites for Linear Applications," IEEE Spectrum, Feb. 1972, p. 26;and March 1972, p. 42.

2. Sommerfeld, A., "Lectures on Theoretical Physics," Electrodynamics, Vol. III, 1948.

3. Jackson, J. D., "Classical Electrodynamics," Library of Congress Catalog Card Number 62-8774.

4. Chomitsch, W. J., "Ferrite Receiver Antennas," Radio und Fernsehen, Vol. 21, 1962; p.660, translated from Gosenergoisdat, Moskow, 1960.

$$\mu_{eff\ rel} = \frac{\mu_{i_{rel}}}{1+(\mu_{i_{rel}}-1).N}$$

theoretical: $N = (\frac{b}{c})^2\left[\frac{a}{2c}\ln\frac{a/c+1}{a/c-1} - 1\right]$ $c^2 = a^2 - b^2$

empirical: $N = 0.84\,(d/l)^{1.7}$

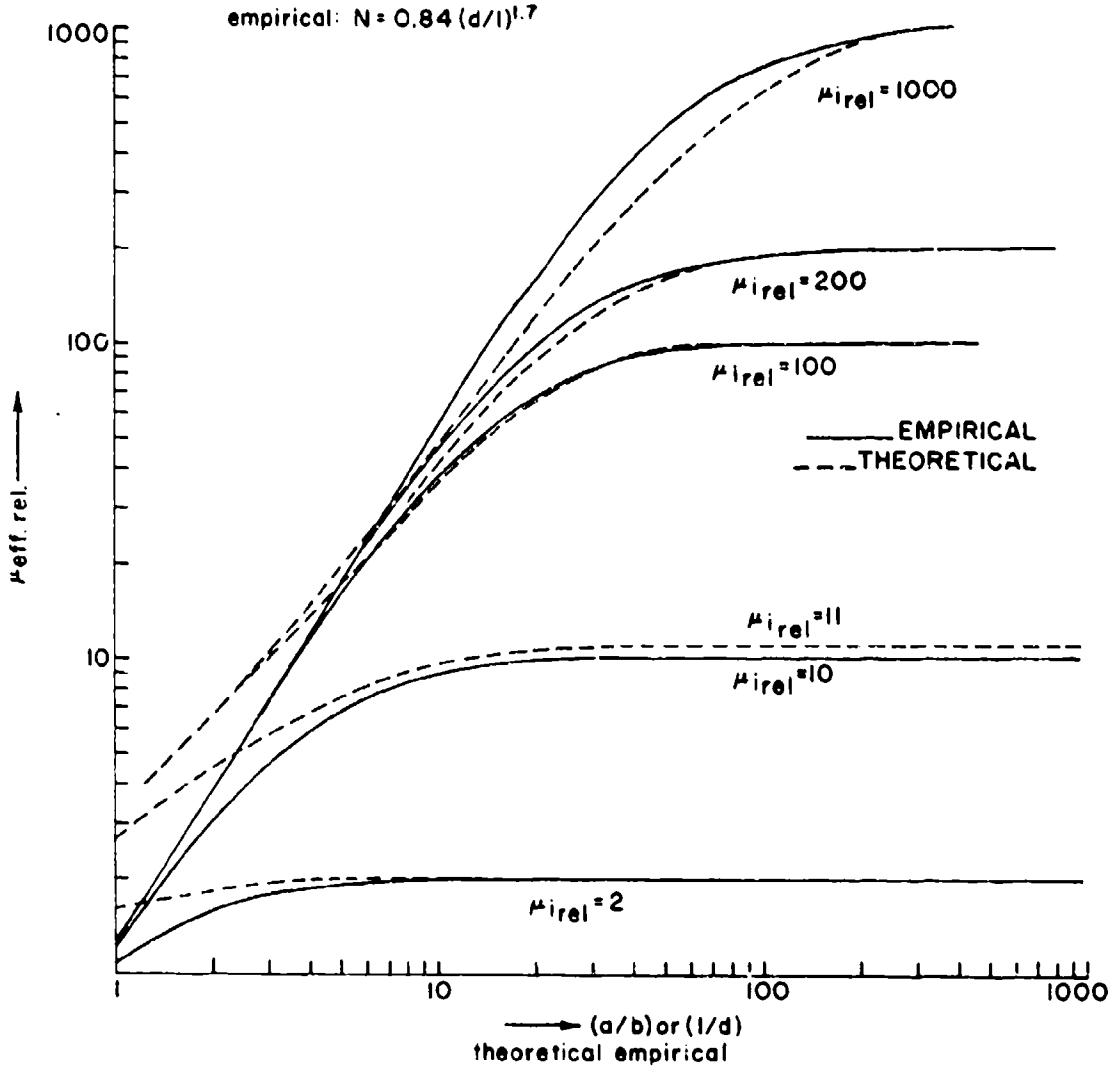

Fig 1 Theoretical and Empirical $\mu_{eff:rel}$ versus length to diameter ratios (a/b) or (l/d)

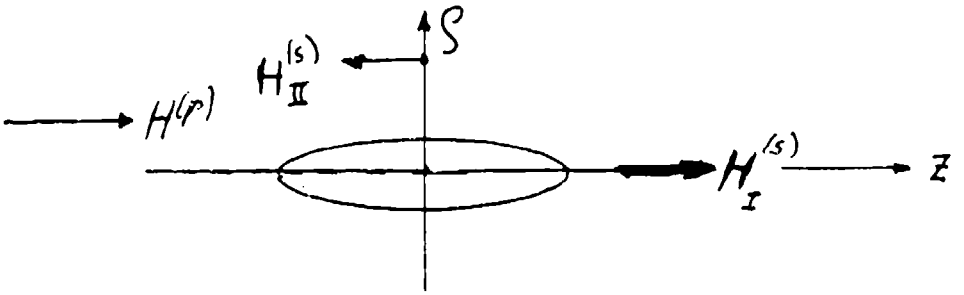

Fig. 2 External Secondary Field Locations I and II

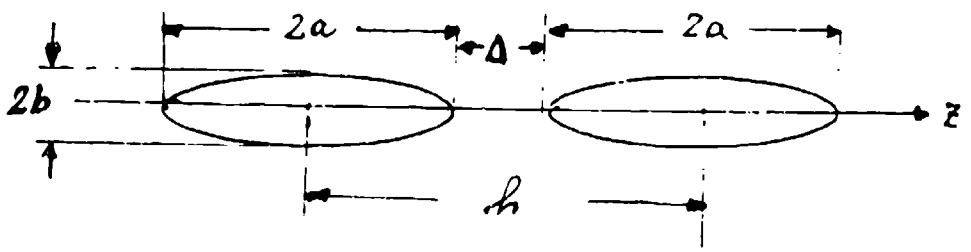

Fig. 3 Two Element Longitudinal Array

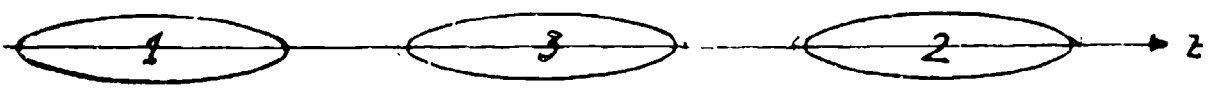

Fig. 4 Three Element Longitudinal Array Designation

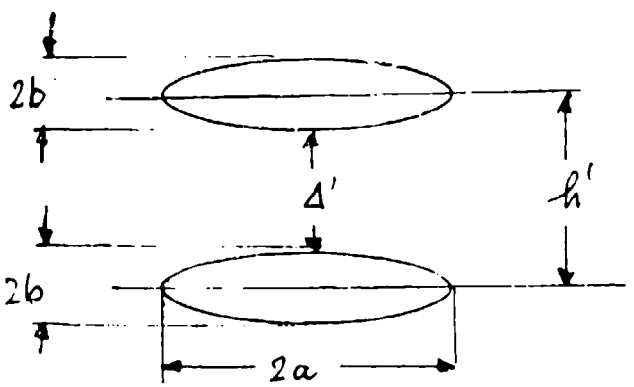

Fig. 5 Two Element Transverse Array Designation

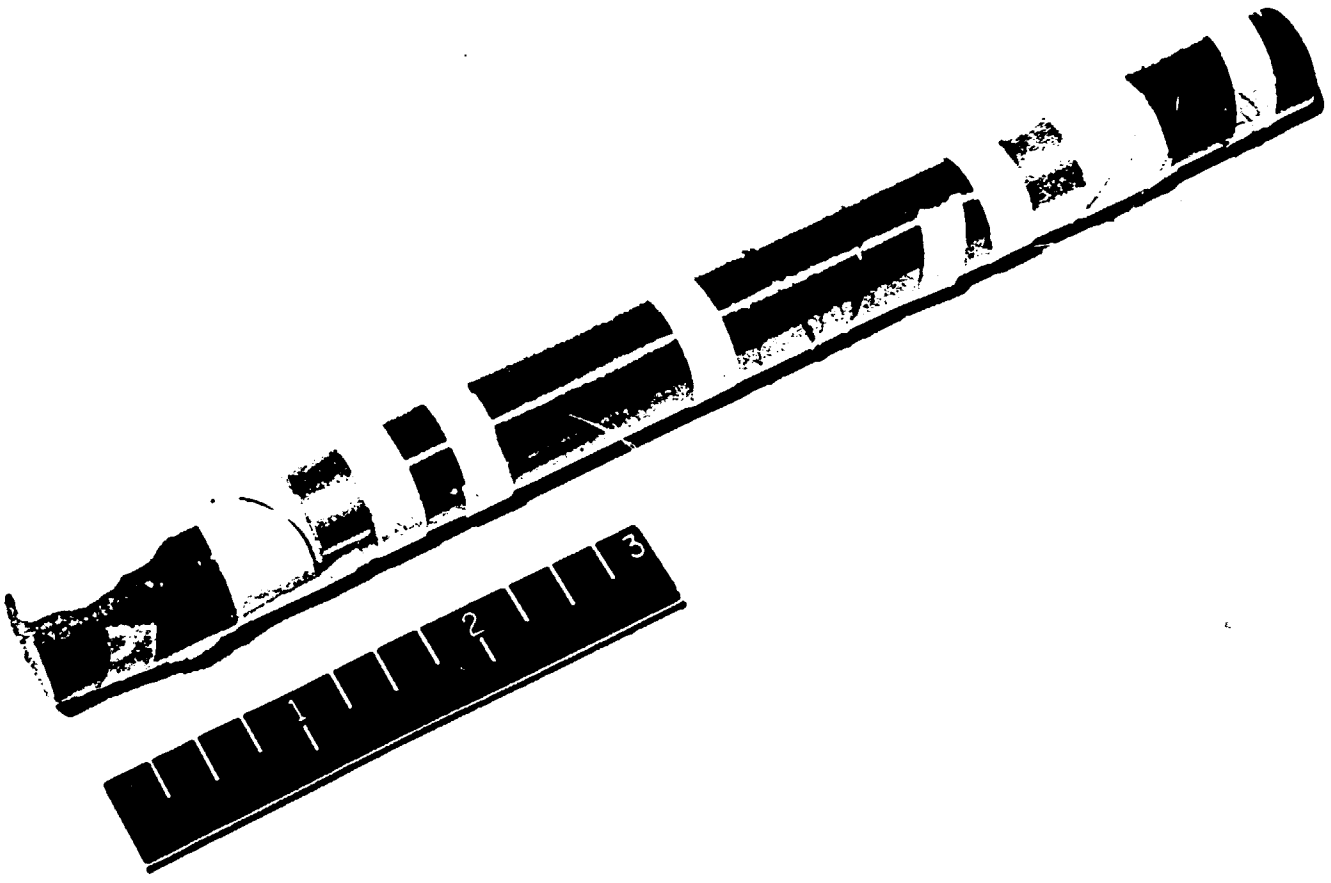

Fig. 6 Ferrite Rod Antenna Array Element

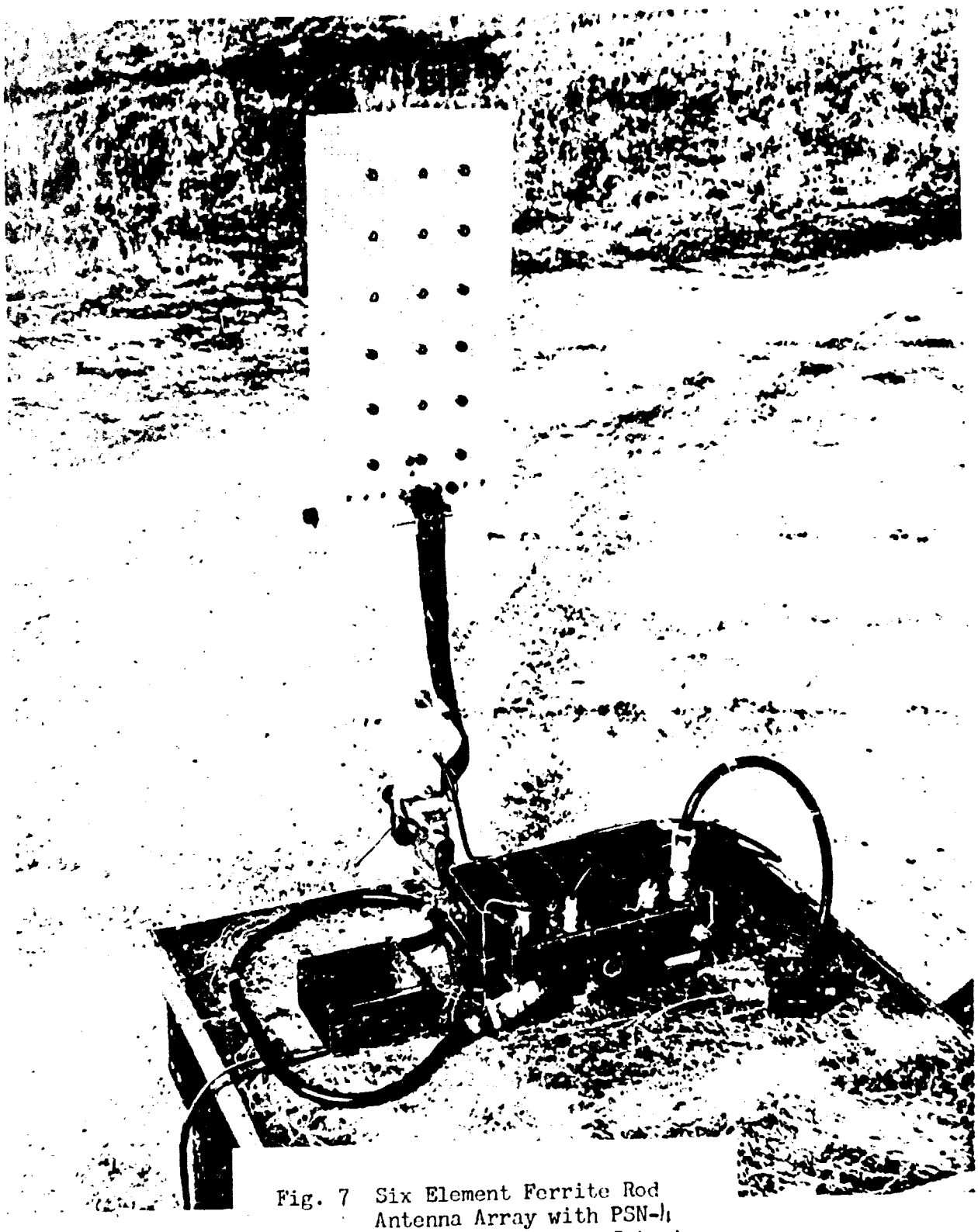

Fig. 7 Six Element Ferrite Rod Antenna Array with PSN-4 Loran-C Navigation Set at Bldg. T113, Evans Area

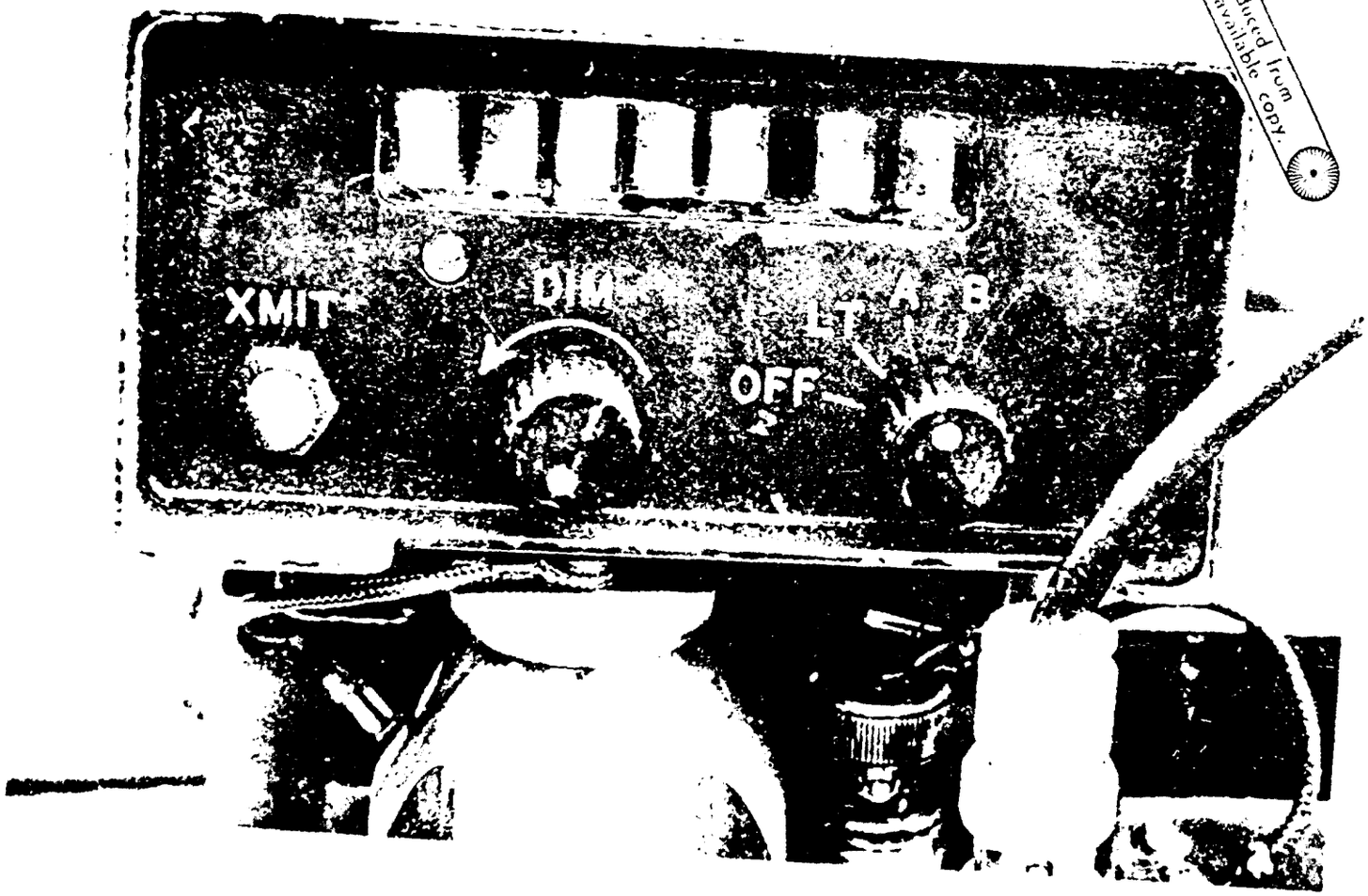

Fig. 8 Close-up View of Time Coordinator Output from PSN-4 Location Set at Fil., Fla., Byrnd Area

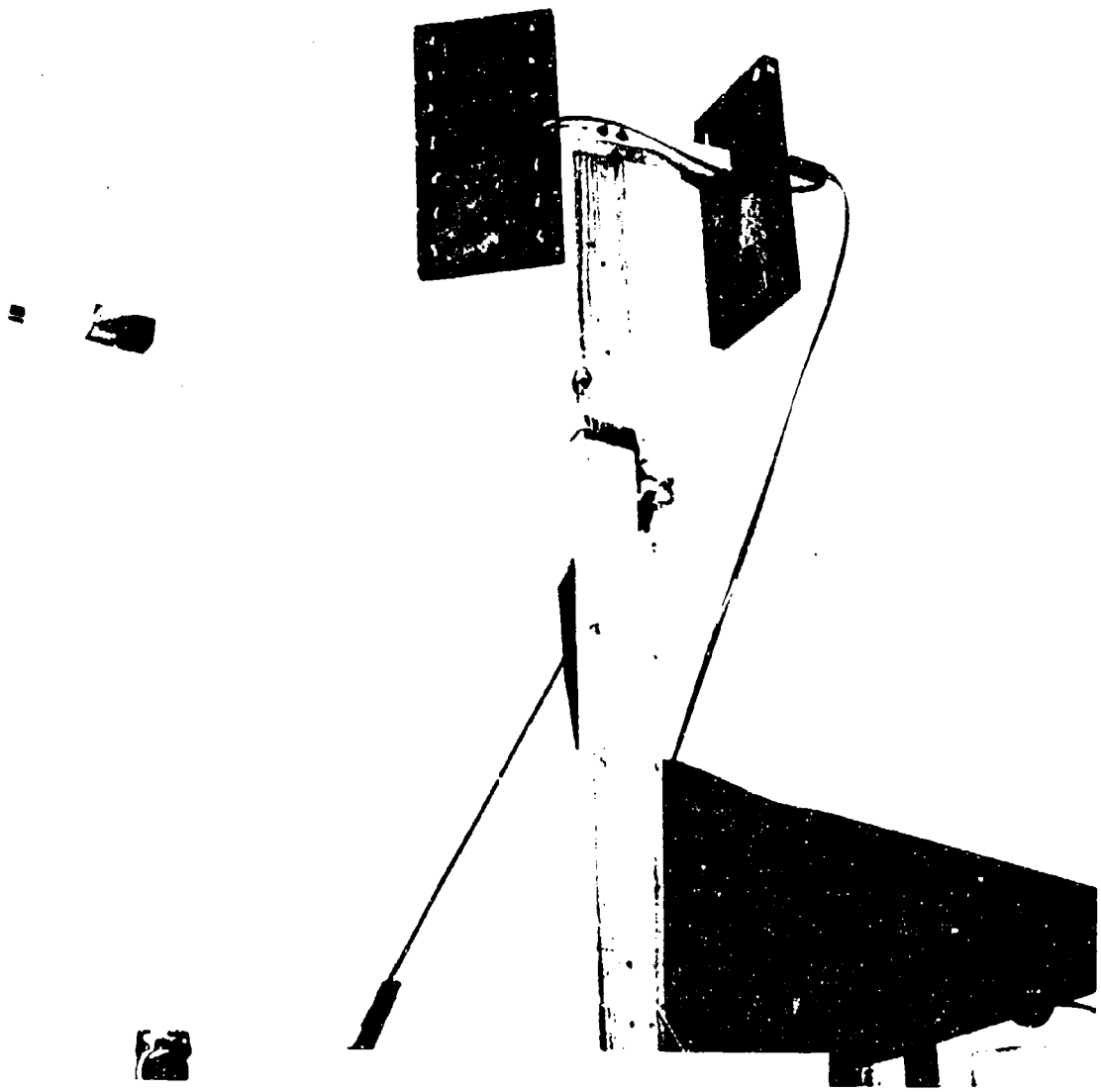

Fig. 9 Twin Transverse Ferrite Rod Antenna Array Mounted on Weapons Carrier

APPENDIX A - MAGNETIZATION OF A FERRITE ELLIPSOID BY A HOMOGENEOUS PRIMARY MAGNETIC FIELD $H^{(p)}$ ALONG THE Z-DIRECTION

The following relations are applicable:

$H = \text{grad}\ \psi$ where ψ the magnetic potential must satisfy the Laplace Differential equation (A.1)

$$div\ grad\ \psi = \Delta\psi = 0 \tag{A.2}$$

inside $\psi^{(i)} = \psi^{(p)} + \psi^{(\alpha)}$ and (A.3)

outside $\psi^{(o)} = \psi^{(p)} + \psi^{(\beta)}$ (A.3')

such that on the boundary surface

$$\psi^{(o)} = \psi^{(i)} \quad \text{and} \tag{A.4}$$

$$\frac{\partial \psi^{(o)}}{\partial n} = \mu_{rel} \frac{\partial \psi^{(i)}}{\partial n} \tag{A.4'}$$

(i.e., surface divergence B=0)

(n normal to boundary surface)

The boundary surface between air and ferrite is defined by Fig. A.1 and the corresponding analytical expressions:

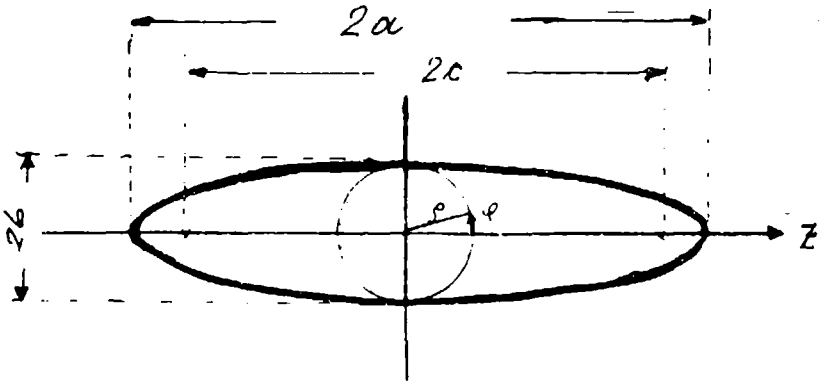

Fig. A.1 - Boundary Surface Between Air and Ferrite

$$\frac{z^2}{a^2} + \frac{x^2+y^2}{b^2} = 1 \qquad \sqrt{x^2+y^2} = \rho^2 \tag{A.5}$$

$$c^2 = a^2 - b^2$$

In terms of elliptical coordinates u, v,

$$z = c \cdot Ch$$

$$\left.\begin{aligned} x &= c \cdot Sh u \cdot \sin v \cdot \cos\varphi \\ y &= c \cdot Sh u \cdot \sin v \cdot \sin\varphi \end{aligned}\right\} \rho = c \cdot Sh u \cdot \sin v \qquad (A.6)$$

the boundary surface is determined by u_0

$$a = c \cdot Ch u_0 \qquad b = c \cdot Sh u_0$$

$$u_0 = Ar\,Ch \frac{a}{c} = Ar\,Sh \frac{b}{c} \qquad (A.7)$$

(u const. represent confocal ellipsoids, v const. represent confocal hyperboloids)

The Laplace operator in generalized coordinates is:

$$\Delta = \sum_{i,j} \frac{1}{\sqrt{g}} \frac{\partial}{\partial q_i} \left[\sqrt{g} \cdot g^{(i,j)} \cdot \frac{\partial}{\partial q_j} \right]. \qquad (A.8)$$

where the g are contained in the square of a path element in q coordinates.

$$(d\bar{s})^2 = \sum_{ij} g_{ij}\, dq^i dq^j = \sum g^{ij} dq_i\, dq_j. \qquad (A.9)$$

corresponding to the dyadic relationship

$$d\bar{s} = d\bar{q} \cdot (\nabla, \bar{s}) \qquad g^{ij} = \frac{d\bar{q}}{ds} = (g_{ij})^{-1}$$

Introduction of Equation (A.9) into (A.6) yields:

$$dz = c \cdot Sh u \cdot \cos v \cdot du - c \cdot Ch u \cdot \sin v \cdot dv \qquad \text{(A.10)}$$

$$dx = c \cdot Ch u \cdot \sin v \cdot \cos\varphi \, du + c\, Sh u \cdot \cos v \cos\varphi \cdot dv - c\, Sh u \cdot \sin v \cdot \sin\varphi \cdot d\varphi$$

$$dy = c \cdot Ch u \cdot \sin v \sin\varphi \cdot du + c\, Sh u \cos v \cdot \sin\varphi\, dv + c \cdot Sh u \cdot \sin v \cdot \cos\varphi \cdot d\varphi$$

$$(d\bar{s})^2 = (dx)^2 + (dy)^2 + (dz)^2 = (ds_u)^2 + (ds_v)^2 + (ds_\varphi)^2 =$$

$$= \underbrace{\left[c^2\left(Sh^2 u + \sin^2 v\right)\right]}_{g_{11}} du^2 + \underbrace{\left[c^2 Sh^2 u + \sin^2 v\right]}_{g_{22}} dv^2 + \underbrace{\left[c^2 \left(Sh u \cdot \sin v\right)^2\right]}_{g_{33}} d\varphi^2$$

$$g_{12} = g_{23} = g_{31} = 0$$

hence: $g^{ii} = \dfrac{1}{g^{ii}} \qquad g = g_{11} g_{22} g_{33}$

$$g^{11} = g^{22} = \frac{1}{c^2\left(Sh^2 u + \sin^2 v\right)} \qquad \text{(A.11)}$$

$$g^{33} = \frac{1}{c^2 \left(Sh u \cdot \sin v\right)^2} \qquad \text{(A.11')}$$

$$\sqrt{g} = c^3 \left(Sh^2 u + \sin^2 v\right)\left(Sh u \cdot \sin v\right) = \frac{1}{g^{11}} \cdot \frac{1}{\sqrt{g^{33}}} \qquad \text{(A.11'')}$$

$$\Delta\psi = \frac{1}{\sqrt{g_{11}\,g_{22}\,g_{33}}}\cdot\left\{\frac{\partial}{\partial u}\left[\sqrt{g_{33}}\,\frac{\partial}{\partial u}\psi\right] + \right.$$

$$+\frac{\partial}{\partial v}\left[\sqrt{g_{33}}\,\frac{\partial}{\partial v}\psi\right] + \qquad (A.12)$$

$$\left. +\frac{\partial}{\partial\varphi}\left[\frac{g_{11}}{\sqrt{g_{33}}}\,\frac{\partial}{\partial\varphi}\psi\right]\right\}$$

where $\frac{\partial}{\partial\varphi} = 0$ for axial symmetry (A.12')

from Equation (A.11) to (A.12')

$$\frac{\partial}{\partial u}\left[Sh u\cdot\sin v\,\frac{\partial\psi}{\partial u}\right] + \frac{\partial}{\partial v}\left[Sh u\cdot\sin v\,\frac{\partial\psi}{\partial v}\right] = 0 \qquad (A.13)$$

A particular solution of Equation (A.13) is the potential of a homogenous field along the z-direction, i.e. proportional to z:

$$\psi^{(\alpha)} = A^{(\alpha)}\cdot c\cdot Ch u\cdot\cos v \qquad (A.14)$$

which is proven by substitution of Equation (A.14) into (A.13)

$$\left[2\,Sh u\,Ch u - 2\,Sh u\,Ch u\right]\sin v\cdot\cos v = 0$$

Another particular solution is obtained by variation of the constant A in form of a function of f (u) which for u_o (i.e., on the surface of the ellipsoid) is a constant.

$$\psi^{(\beta)} = f(u)\cdot\cos v \qquad (A.15)$$

$$\frac{\partial}{\partial u}\left[Sh u\cdot\sin v\cdot\frac{df}{du}\cdot\cos v\right] - \frac{\partial}{\partial v}\left[Sh u\cdot\sin v\cdot f(u)\cdot\sin v\right] = 0$$

$$\sin v \cdot \cos v \left[Ch u \cdot \frac{df}{du} + Sh u \frac{d^2 f}{du^2} - 2 Sh u \cdot f \right] = 0 \qquad \text{(A.16)}$$

set: $$f(u) = U(u) \cdot Ch u \qquad \text{(A.16')}$$

from Equations (A.16) and (A.16')

$$Ch^2 u \cdot \frac{dU}{du} + Ch u \cdot Sh u \cdot U +$$

$$+ Sh u \cdot \left[\frac{d^2 U}{du^2} \cdot Ch u + 2 \frac{dU}{du} \cdot Sh u + U \cdot Ch u \right] +$$

$$- 2 \cdot Sh u \cdot Ch u \cdot U = 0$$

$$\frac{dU}{du} \left[Ch^2 u + 2 Sh^2 u \right] + \frac{d^2 U}{du^2} \cdot Sh u \cdot Ch u = 0$$

$$\frac{U''}{U'} = \frac{Ch^2 u + Sh^2 u}{Sh u \cdot Ch u} = \frac{1}{Th u} + 2 Th u \qquad \text{(A.17)}$$

$$\frac{d}{du} \cdot \ln U' = \frac{1}{Th u} + 2 Th u$$

$$\ln U' = \int Ch u \cdot du + 2 \int Th u \cdot du =$$

$$= - \ln Sh u - 2 \ln Ch u =$$

$$= \ln \frac{1}{(Sh u) \cdot (Ch u)^2} \qquad \text{(A.18)}$$

$$u' = \frac{A^{(\beta)} \cdot c}{Shu \cdot (chu)^2}$$ where: $A^{(\beta)} \cdot c$ = integration constant

$$u = A^{(\beta)} \cdot c \int \frac{du}{Shu \cdot (chu)^2} = A^{(\beta)} c \cdot \left[\frac{Thu}{Shu} + \int \frac{Thu \cdot chu}{(Shu)^2} du \right] =$$

$$= \frac{A^{(\beta)} c}{chu} + A^{(\beta)} \cdot c \int \frac{du}{Shu} = \frac{A^{(\beta)} c}{chu} + A^{(\beta)} c \cdot \ln\left(j Th \frac{u}{2}\right) + C =$$

$$= \frac{A^{(\beta)} c}{chu} + A^{(\beta)} c \ln\left(j \sqrt{\frac{chu-1}{chu+1}}\right) + C \qquad \text{(A.19)}$$

$$u = \frac{A^{(\beta)} c}{chu} + \frac{1}{2} \ln \frac{chu-1}{chu+1} + \underbrace{\left[A^{(\beta)} c \cdot j \frac{\pi}{2} + C \right]}_{K \cdot c}$$

from Equations (A.19), (A.16'), and (A.15)

$$\psi^{(\beta)} = \underbrace{K \cdot c \cdot chu \cdot \cos v}_{\text{already used particular solution Equation (A.14) so that only the second term is a new particular solution.}} + A^{(\beta)} \cdot c \left[1 + \frac{chu}{2} \ln \frac{chu-1}{chu+1} \right] \cdot \cos v \qquad \text{(A.20)}$$

From Equation (A.14)

$$\psi^{(\alpha)} = A^{(\alpha)} \cdot c \cdot chu \cdot \cos v \qquad \text{(A.21)}$$

and Equation (A.20)

$$\psi^{(\beta)} = A^{(\beta)} \cdot c \left[1 + \frac{chu}{2} \cdot \ln \frac{chu-1}{chu+1} \right] \cdot \cos v \qquad \text{(A.22)}$$

satisfy the Laplace Differential equation.

$\psi^{(\alpha)}$ represents the potential of a homogeneous field like the primary field

$\psi^{(\beta)}$ represents the secondary potential outside.

From Equations (A.3) and (A.21)

$$\psi^{(i)} = \psi^{(\alpha)} + \psi^{(p)} = \underbrace{\left[H^{(p)} - A^{(\alpha)}\right]}\, c \cdot \mathrm{ch}u \cdot \cos v = H_z^{(i)} \cdot c \cdot \mathrm{ch}u \cdot \cos v \qquad \text{(A.23)}$$

from Equations (A.3) and (A.22')

$$\psi^{(o)} = \psi^{(\beta)} + \psi^{(p)} = H^{(p)} \cdot c \cdot \mathrm{ch}u \cdot \cos v - A^{(\beta)} \cdot c \cdot \cos v \left[1 + \frac{\mathrm{ch}u}{2} \cdot \ln \frac{\mathrm{ch}u - 1}{\mathrm{ch}u + 1}\right] \qquad \text{(A.24)}$$

the choice of sign of $A^{(\alpha)}, A^{(\beta)}$ in the superposition of primary and secondary potentials was made for reasons of physical consistency with the concepts of magnetization.

In connection with the boundary conditions Equation (A.24), the relations Equation (A.10') are needed:

$$(ds)_u = \sqrt{g_{11}} \cdot du = c \sqrt{\mathrm{sh}^2 u + \sin^2 v} \cdot du$$

$$(ds)_v = \sqrt{g_{22}} \cdot dv = c \sqrt{\mathrm{sh}^2 u + \sin^2 v} \cdot dv \qquad \text{(A.25)}$$

$$\frac{\partial \psi}{\partial s_u} = \frac{1}{c\sqrt{\mathrm{sh}^2 u + \sin^2 v}} \cdot \frac{\partial \psi}{\partial u} = \frac{1}{c\sqrt{\mathrm{ch}^2 u - \cos^2 v}} \cdot \frac{\partial \psi}{\partial u}$$

$$\frac{\partial \psi}{\partial s_v} = \frac{1}{c\sqrt{\mathrm{Sh}^2 u + \sin^2 v}} \cdot \frac{\partial \psi}{\partial v} = \frac{1}{c\cdot\sqrt{\mathrm{Ch}^2 u - \cos^2 v}} \cdot \frac{\partial \psi}{\partial v} \qquad (A.25')$$

$$\frac{\partial \psi^{(i)}}{\partial u} = H^{(i)} \cdot c \cdot \mathrm{Sh}u \cdot \cos v$$

$$\frac{\partial \psi^{(i)}}{\partial v} = -H^{(i)} \cdot c \cdot \mathrm{Ch}u \cdot \sin v$$

$$\frac{\partial \psi^{(\beta)}}{\partial u} = A^{(\beta)} \cdot c \cdot \cos v \cdot \left[\frac{\mathrm{Sh}u}{2} \cdot \ln\frac{\mathrm{Ch}u - 1}{\mathrm{Ch}u + 1} + \frac{\mathrm{Ch}u}{\mathrm{Sh}u}\right] \qquad (A.26)$$

$$\frac{\partial \psi^{(\beta)}}{\partial v} = -A^{(\beta)} \cdot c \cdot \sin v \cdot \left[1 + \frac{\mathrm{Ch}u}{2} \ln\frac{\mathrm{Ch}u - 1}{\mathrm{Ch}u + 1}\right] \qquad (A.26')$$

Substitution of Equation (A.25) to (A.26'), Equation (A.7) into (A.4) and (A.4') yields:

$$H^{(i)} \cdot a \cdot \cos v = H^{(p)} \cdot a \cdot \cos v - A^{(\beta)} \cdot c \cdot \cos v \cdot \left[1 + \frac{a}{2c} \ln \frac{a/c - 1}{a/c + 1}\right]$$

$$\frac{\mu_{rel} \cdot H^{(i)} \cdot b \cdot \cos v}{c\sqrt{(a/c)^2 - \cos^2 v}} = \frac{1}{c\sqrt{(a/c)^2 - \cos^2 v}} \cdot \left\{ H^{(p)} \cdot b \cdot \cos v - \right.$$

$$\left. - A^{(\beta)} \cdot c \cdot \cos v \cdot \left[\frac{b/c}{2} \ln \frac{a/c - 1}{a/c + 1} + \frac{a}{b}\right]\right\}$$

$$H^{(p)} = H^{(i)} + A^{(\beta)} \cdot \frac{c}{a}\left[1 + \frac{a}{2c} \ln \frac{a/c - 1}{a/c + 1}\right] \quad \Big| \cdot (-1)$$

$$H^{(p)} = \mu_{rel} H^{(i)} + A^{(\beta)} \cdot \frac{c}{b}\left[\frac{b}{2c} \ln \frac{a/c - 1}{a/c + 1} + \frac{a}{b}\right]$$

$$0 = (\mu_{rel} - 1) H^{(i)} + A^{(\beta)}\left[\frac{a \cdot c}{b^2} - \frac{c}{a}\right]$$

$$H^{(i)} = -\frac{A^{(\beta)}}{(\mu_{rel} - 1)} \cdot \frac{c^3}{b^2 a} = -\frac{A^{(\beta)}}{\chi} \cdot \frac{c^3}{b^2 a} \qquad \text{(A.27)}$$

$$A^{(\beta)} = -\frac{H^{(p)} \chi \cdot \frac{b^2 a}{c^3}}{1 - \chi\left(\frac{b}{c}\right)^2\left[1 + \frac{a}{2c} \ln \frac{a/c - 1}{a/c + 1}\right]} \qquad \text{(A.28)}$$

from Equation (A.27) and (A.28)

$$H^{(i)} = + \frac{H^{(p)}}{1 - \chi\left(\frac{b}{c}\right)^2 \cdot \left[1 + \frac{a}{2c} \cdot \ln \frac{a/c - 1}{a/c + 1}\right]} = \tag{A.29}$$

$$= \frac{H^{(p)}}{1 + \chi N} \qquad \text{where}$$

$$N = \left(\frac{b}{c}\right)^2 \cdot \left[\frac{a}{2c} \cdot \ln \frac{a/c + 1}{a/c - 1} - 1\right] \tag{A.29'}$$

from Equation (A.28) and (A.24)

$$\varphi^{(o)} = H^{(p)} \cdot c \cdot \cos v \cdot \left[\cosh u + \frac{\chi \cdot \frac{b^2 a}{c^3} \left[1 + \frac{\cosh u}{2} \ln \frac{\cosh u - 1}{\cosh u + 1}\right]}{1 - \chi\left(\frac{b}{c}\right)^2 \cdot \left[1 + \frac{a}{2c} \cdot \ln \frac{a/c - 1}{a/c + 1}\right]} \right] =$$

$$= \varphi^{(p)} + \varphi^{(s)} \tag{A.30}$$

where $\varphi^{(p)}$ is the primary potential and $\varphi^{(s)}$ the secondary potential. The outside secondary field along the z-axes involves

$$H_{zI}^{(s)} = \left[\frac{\partial}{\partial s_u} \varphi^{(s)}\right]_{\text{for } v = 0} \tag{A.31}$$

for the z-component

and $H_{\rho I}^{(s)} = \left[\frac{\partial}{\partial s_v} \varphi^{(s)}\right]_{\text{for } v = 0} = 0$ for the ρ-component which is zero because of $\sin v$

The outside secondary field along the ρ axis involves:

$$H_{z\,II}^{(s)} = \left[\frac{\partial}{\partial z}\psi^{(s)}\right]_{\text{for } v=\frac{\pi}{2}} \qquad \text{(A.31')}$$

for the z-component

and $H_{\rho\,II}^{(s)} = \left[\frac{\partial}{\partial \rho}\psi^{(s)}\right]_{\text{for } v=\frac{\pi}{2}} = 0$ for the ρ -component which is zero because of $\cos v$

Fig. A.2 illustrates the situation:

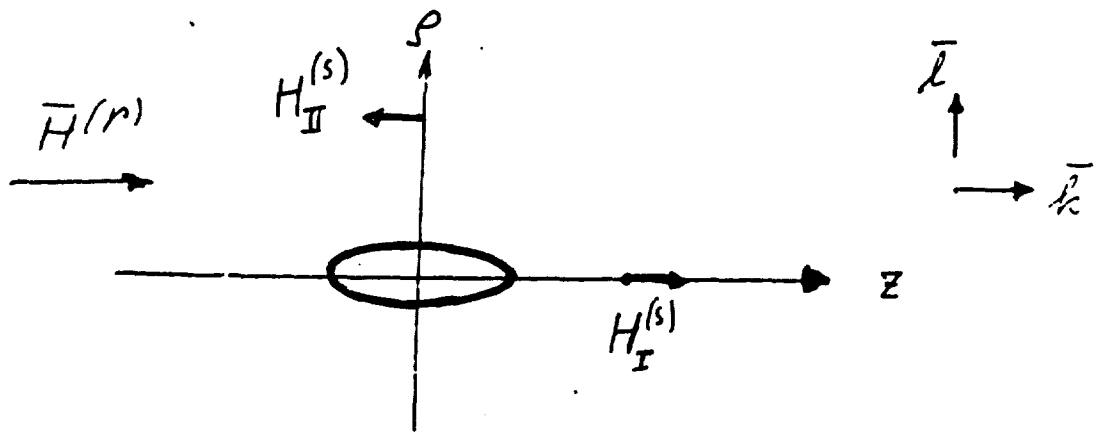

Fig. A.2 - Field Distribution

From Equations (A.31), (A.30), (A.25) and (A.26'), (A.6), (A.7)

$$H_I^{(s)} = \frac{|A^{(i)}|\cdot c}{c\sqrt{ch^2u-1}}\left[\frac{shu}{2}\ln\frac{chu-1}{chu+1} + \frac{chu}{shu}\right] =$$

$$= \frac{|A^{(i)}|}{\sqrt{\left(\frac{z}{c}\right)^2-1}}\left[\frac{\sqrt{\left(\frac{z}{c}\right)^2-1}}{2}\cdot\ln\frac{|z/c|-1}{|z/c|+1} + \frac{|z/c|}{\sqrt{(z/c)^2-1}}\right] =$$

$$H_I^{(s)} = |A^{(p)}| \cdot \left\{ \frac{|z/c|}{(\frac{z}{c})^2 - 1} + \frac{1}{2} \cdot \ln \frac{|z/c| - 1}{|z/c| + 1} \right\} \qquad (A.32)$$

similarly

$$H_{II}^{(s)} = \frac{|A^{(p)}| \cdot c}{c \operatorname{ch} u} \cdot \left\{ (-1) \cdot \left[1 + \frac{\operatorname{ch} u}{2} \cdot \ln \frac{\operatorname{ch} u - 1}{\operatorname{ch} u + 1} \right] \right\} =$$

$$= \frac{|A^{(p)}|}{\sqrt{1 + \operatorname{sh}^2 u}} \cdot (-1) \cdot \left\{ 1 + \frac{\sqrt{1 + \operatorname{sh}^2 u}}{2} \cdot \ln \frac{\sqrt{1 + \operatorname{sh}^2 u} - 1}{\sqrt{1 + \operatorname{sh}^2 u} + 1} \right\} =$$

$$= -\frac{|A^{(p)}|}{\sqrt{1 + (s/c)^2}} \cdot \left\{ 1 + \frac{\sqrt{1 + (s/c)^2}}{2} \cdot \ln \frac{\sqrt{1 + (s/c)^2} - 1}{\sqrt{1 + (s/c)^2} + 1} \right\} \qquad (A.32')$$

from Equation (A.32) and (A.28) (A.33 and A.33')

$$H_I^{(s)} = \frac{H^{(p)} \cdot \chi \cdot \frac{b^2 a}{c^3}}{1 + \chi (\frac{b}{c})^2 \left[\frac{a}{2c} \ln \frac{a/c + 1}{a/c - 1} - 1 \right]} \left\{ \frac{|z/c|}{(z/c)^2 - 1} + \frac{1}{2} \ln \frac{|z/c| - 1}{|z/c| + 1} \right\}$$

from Equation (A.32') and (A.28)

$$H_{II}^{(s)} = -\frac{H^{(p)} \cdot \chi \cdot \frac{b^2 a}{c^3}}{1 + \chi (\frac{b}{c})^2 \left[\frac{a}{2c} \ln \frac{a/c + 1}{a/c - 1} - 1 \right]} \cdot \left\{ \frac{1}{\sqrt{1 + (s/c)^2}} + \frac{1}{2} \ln \frac{\sqrt{1 + (s/c)^2} - 1}{\sqrt{1 + (s/c)^2} + 1} \right\}$$

Approximations for Equation (A.33) and (A.33'): can be introduced for:

$(z/c) = f \gg 1$ using the series expansion for the natural log term with $r \ll 1$

$$\ln(1+r) = r - \frac{r^2}{2} + \frac{r^3}{3} - \frac{r^4}{4} + \frac{r^5}{5} + \cdots$$

$$\ln(1-r) = -r - \frac{r^2}{2} - \frac{r^3}{3} - \frac{r^4}{4} - \frac{r^5}{5} - \cdots$$

$$\frac{1}{2}\cdot\ln\frac{(1-r)}{1+r} = -r - r^3/3 - r^5/5 - \cdots$$

$$r \longrightarrow \frac{1}{f}$$

from Equation (A.33)

$$\left\{\frac{f}{f^2-1} - \frac{1}{f} - \frac{1}{3f^3} \cdots\right\} f = \frac{1}{f\left[1-\frac{1}{f^2}\right]} - \frac{1}{f} - \frac{1}{3f^3} =$$

$$\doteq \frac{1+\frac{1}{f^2}}{f} - \frac{1}{f} - \frac{1}{3f^3} = \frac{1}{f^3} - \frac{1}{3f^3} \doteq \left|\frac{2}{3f^3}\right| \qquad \text{(A.33a)}$$

from Equation (A.33') similarly

$$\rho/c = \eta \gg 1 \; ; \quad f \longrightarrow \sqrt{1+\eta^2}$$

$$\frac{1}{\sqrt{1+\eta^2}} - \frac{1}{\sqrt{1+\eta^2}} - \frac{1}{3\left[\sqrt{1+\eta^2}\right]^3} \doteq \frac{1}{3\eta^3} \qquad \text{(A.33b)}$$

from Equation (A.33a) and (A.33)

$$z H_I^{(s)} \overset{|z/c|\gg 1}{=} \frac{H^{(p)} \chi \cdot \frac{b^2 a}{c^3}}{1+\chi N} \cdot \left| \frac{2}{3\zeta^3} \right| = \frac{H^{(p)} \chi 2 b^2 a}{3(1+\chi N)} \cdot \frac{1}{|z|^3} \qquad \text{(A.34)}$$

from Equation (A.33b) and (A.33')

$$z H_{II}^{(s)} \overset{|s/c|\gg 1}{=} - \frac{H^{(p)} \chi \frac{b^2 a}{c^3}}{1+\chi N} \cdot \left| \frac{1}{3\eta^2} \right| = - \frac{H^{(p)} \chi b^2 a}{3(1+\chi N)} \cdot \frac{1}{|s|^3} \qquad \text{(A.34')}$$

Equation (A.34) and (A.34') exhibit the distance dependency of a magnetic dipole field as shown below in Fig. A.3.

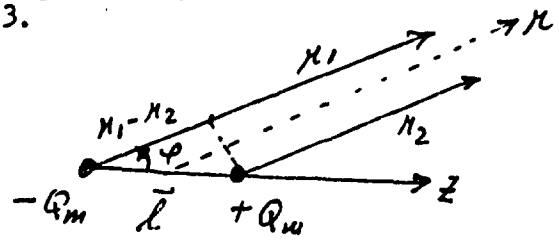

Fig. A.3 - Dipole Geometry

$$\varphi_D = \frac{Q_m}{4\pi\mu_0} \cdot \left[\frac{1}{r_1} - \frac{1}{r_2} \right] =$$

$$= \frac{Q_m}{4\pi\mu_0} \cdot \frac{r_2 - r_1}{r_1 r_2} \doteq \frac{Q_m \cdot l \cdot \cos\varphi}{4\pi\mu_0 r^2} \qquad \text{(A.35)}$$

$Q_m \cdot l = M$ is the dipole moment.

$$H_r = -\frac{\partial \varphi_D}{\partial r} \doteq \frac{M}{4\pi\mu_0} \cdot \frac{2\cos\varphi}{r^3} \qquad \text{(A.35')}$$

$$H_\varphi = -\frac{1}{r} \frac{\partial \varphi_D}{\partial \varphi} \doteq \frac{M}{4\pi\mu_0} \cdot \frac{\sin\varphi}{r^3} \qquad \text{(A.35'')}$$

Equation (A.35') for $\varphi = 0$;
and (A.34)

$$ {}_z H_I = \frac{|m_z|}{2\pi \mu_0 |z|^3} \overset{!}{=} \frac{H^{(p)} \cdot \chi}{1 + \chi N} (b^2 a) \cdot \frac{2}{3} \frac{1}{|z|^3} \qquad \text{(A.36)} $$

Equation (A.35'') for $\rho = \frac{\pi}{2}$ and (A.34')

$$ {}_z H_{II} = -\frac{|m_z|}{4\pi \mu_0 |\rho|^3} \overset{!}{=} -\frac{H^{(p)} \cdot \chi}{1 + \chi N} \cdot (b^2 a) \cdot \frac{1}{3} \cdot \frac{1}{|\rho|^3} \qquad \text{(A.36')} $$

which yields by comparison:

$$ m_z = \underbrace{\frac{4\pi}{3}(b^2 a)}_{Vol} \cdot \frac{\chi}{1 + \chi N} \cdot \mu_0 H^{(p)} \cdot {}_z P_m \qquad \text{(A.37)} $$

(in the technical rationalized system $[Vol] = m^3$; $[{}_z P_m] = \frac{Volt \cdot sec}{m^2}$

P_m is the magnetic polarization or short the magnetization in accordance with the familiar concept expressed by the B-H diagram in Fig. A.4.

$$ \underbrace{\mu_0 H^{(p)}}_{B^{(p)}} = \mu_0 H^{(i)} + N \cdot P_m (H^{(i)}) \qquad \text{(A.38)} $$

$$ B^{(i)} = \mu_0 H^{(i)} + P_m (H^{(i)}) \qquad \text{(A.38')} $$

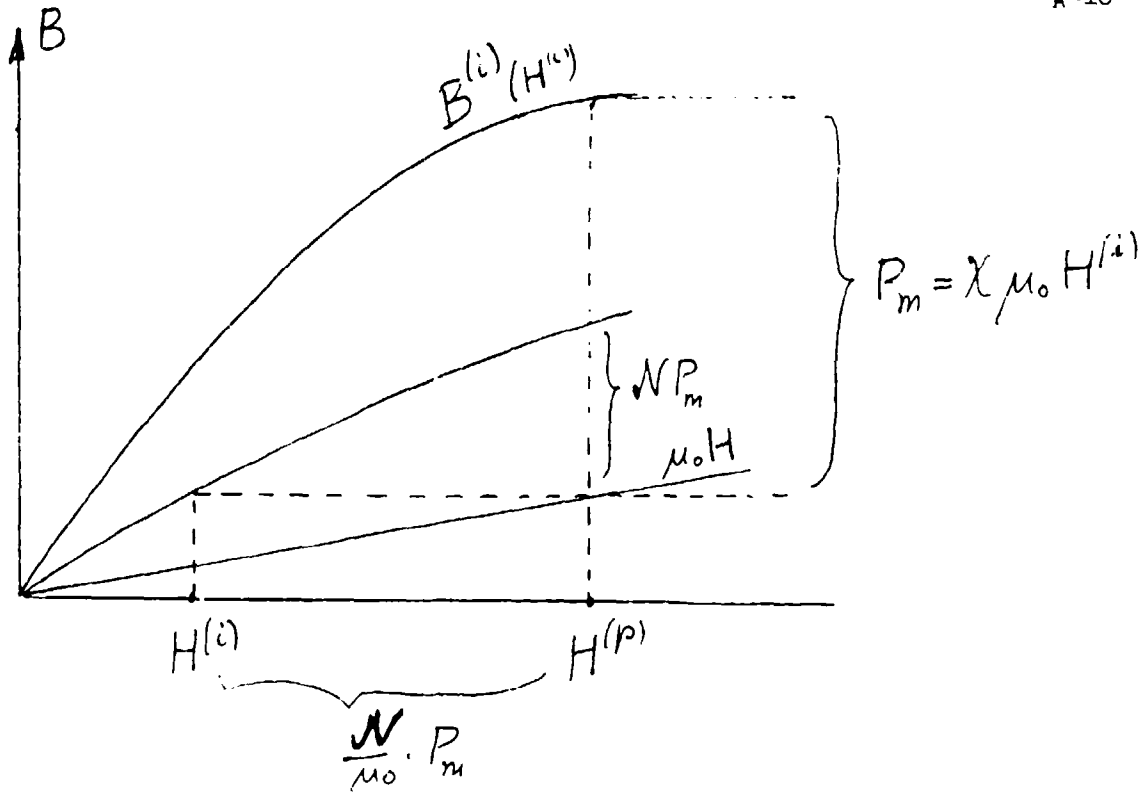

Fig. A.4 - B-H Diagram

one recognizes by comparison with Equation (A.23)

$$A^{(\alpha)} \simeq H^{(p)} - H^{(i)} = \frac{N}{\mu_0} \cdot P_m \qquad (A.38'')$$

The total outside field in positions I (along the z-axis) is

$$H_I^{(o)} = H_z^{(p)} + {}_z H_I^{(s)} \qquad (A.39)$$

The total outside field in positions II (along the z-axis is)

$$H_{II}^{(o)} = H_z^{(p)} - |{}_z H_{II}^{(s)}| \qquad (A.39')$$

APPENDIX B - INSERTION OF A SECOND ELLIPSOID OF FERRITE INTO THE COMPOSITE FIELD PRODUCED BY THE FIRST ELLIPSOID (LONGITUDINAL ARRAY)

Fig. B.1 illustrates the situation.

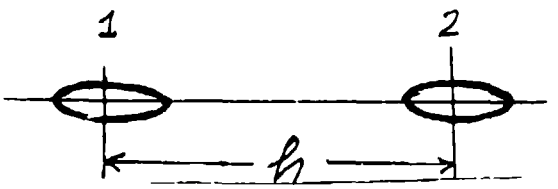

Fig. B.1 - Two Element Longitudinal Array

(1 and 2 are of the same material and have the same dimensions)

The second ellipsoid has as its primary field now that described by Equation (A.39) and (A.33) or approximately (A.34). This field is not homogeneous anymo anymore. For materials with intrinsically large permeability homogeneous magnetization can be assued however; so that the approach is permissible:

$$ {}_oH_2^{(i)} = \frac{H_I^{(o)}}{1+\chi N} \tag{B.1} $$

The field inside 2 is then analogous to Equation (A.29)

$$ {}_oH_2^{(i)} = \frac{H_z^{(p)}}{1+\chi N}\left[1 + \frac{\chi \frac{b^2 a}{c^3}}{1+\chi N}\left(\frac{|h/c|}{(h/c)^2-1} + \frac{1}{2}\ln\frac{|h/c|-1}{|h/c|+1}\right)\right] $$

and since $\left|\frac{h}{c}\right| \gg 1$ the approach in Equation (A.33a) is permissible:

$$ {}_oH_2^{(i)} = \frac{H_z^{(p)}}{1+\chi N}\left[1 + \frac{\chi b^2 a}{1+\chi N}\cdot\frac{2}{3|h|^3}\right] \tag{B.2} $$

This ${}_0H_2^{(i)}$ is associated with a magnetic polarization of 2 which follows from Equation (A.38') as:

$$\frac{1}{\mu_0}({}_0P_2) = \chi H_2^{(i)} = \frac{\chi \cdot H_2^{(p)}}{1+\chi N}\cdot\left[1+\frac{\chi b^2 a}{1+\chi N}\cdot\frac{2}{3|h|^3}\right] \qquad (B.2')$$

This polarization produces a secondary field at the location of 1 analogous to Equation (A.36) and (A.37).

$$H_I^{(s_2)} = \frac{2}{3}\frac{b^2 a}{|h|^3}\cdot\frac{\chi H_2^{(p)}}{1+\chi N}\cdot\left[1+\frac{\chi b^2 a}{1+\chi N}\cdot\frac{2}{3|h|^2}\right] \qquad (B.2'')$$

which produces an additional internal field in 1

$$H_1^{(i)_{s_2}} = \frac{H_I^{(s_2)}}{1+\chi N} \qquad (B.3)$$

so the total new internal field in 1 is

$$H_1^{(i)} = \frac{H_2^{(p)}}{1+\chi N}\cdot\left[1+\frac{2}{3}\frac{b^2 a}{|h|^3}\cdot\frac{\chi}{1+\chi N}\left[1+\frac{\chi b^2 a}{1+\chi N}\cdot\frac{2}{3|h|^3}\right]\right] \qquad (B.4)$$

producing there a

$$\frac{1}{\mu_0}({}_0P_1) = \frac{\chi H_2^{(p)}}{1+\chi N}\cdot\left[1+\frac{2}{3}\frac{b^2 a}{|h|^3}\cdot\frac{\chi}{1+\chi N}\left[1+\frac{\chi b^2 a}{1+\chi N}\cdot\frac{2}{3|h|^3}\right]\right] \qquad (B.5)$$

This corrected magnetization of 1 leads to a new secondary field from 1 at the location of 2; and, therefore, to a new total field at the location of 2 which is analogous to Equation (A.39),

$$H^{(0)}_{1,2} = H_2^{(p)} \cdot \left\{ 1 + \frac{2b^2 a}{3|h|^3} \cdot \frac{\chi}{1+\chi N} \cdot \left[1 + \right. \right. \tag{B.6}$$

$$\left. \left. + \frac{2b^2 a}{3|h|^3} \cdot \frac{\chi}{1+\chi N} \cdot \left(1 + \frac{2b^2 a}{3|h|^3} \cdot \frac{\chi}{1+\chi N} \right) \right] \right\}$$

and, therefore, a new internal field in 2

$$H_2^{(i)}{}_{1,2} = \frac{1}{1+\chi N} \cdot H_I^{(0)}{}_{1,2} \tag{B.6'}$$

and so on in an iterative way which leads to finally

$$H_2^{(i)} = \frac{H_2^{(p)}}{1+\chi N} \cdot \left\{ \sum_{n=0}^{\infty} (S)^n \right\} \tag{B.7}$$

where $S = \frac{2b^2 a}{3|h|^3} \cdot \frac{\chi}{1+\chi N}$ in a geometric progression

$$\left(h \gg c \; ; \; b > a \; ; \; \left(\frac{a}{c}\right)^2 - \left(\frac{b}{c}\right)^2 = 1 \; ; \; S < 1 \right)$$

and, therefore, approximately

$$H_2^{(i)} = H_1^{(i)} = \frac{H_z^{(p)}}{1+\chi N} \cdot \frac{1}{1-\frac{2b^2a}{3|h|^3}\cdot\frac{\chi}{1+\chi N}} \qquad (B.8)$$

the field inside the ferrite body 1 and 2 as the function of distance h between centers.

and the final magnetization is

$$P_2 = P_1 = \frac{\mu_0 \chi H_z^{(p)}}{(1+\chi N)} \cdot \frac{1}{\left[1-\frac{2b^2a}{|h|^3}\cdot\frac{\chi}{1+\chi N}\right]} \qquad (B.9)$$

The validity of this approach is constraint by

$$\frac{2b^2a}{3|h|^3}\cdot\frac{\chi}{1+\chi N} \ll 1$$

APPENDIX C - INSERTION OF A THIRD ELLIPSOID IN BETWEEN TWO OTHER ELLIPSOIDS

Fig. C.1 illustrates the situations.

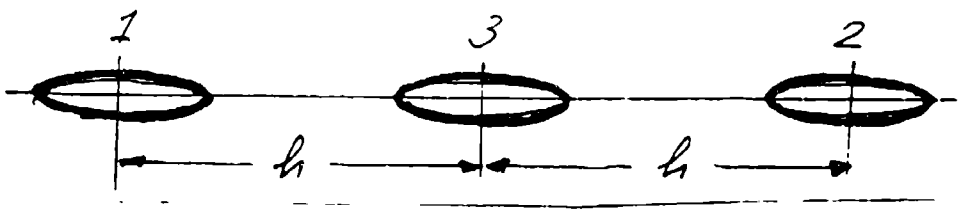

Fig. C.1 - Three Element Longitudinal Array

Fully analogous to App. B, Ferrite Ellipsoid 3 experiences an initial magnetization by the primary field and the secondary fields of 1 and 2. Hence

$$ {}_oP_3 = \frac{\mu_0 \chi H_z^{(p)}}{1+\chi N} + 2\,\frac{2b^2 a}{3|h|^3}\cdot {}_oP_1 \cdot \frac{\chi}{1+\chi N} \qquad (C.1) $$

where ${}_oP_1$ is given by the initial

$$ {}_oP_1 = {}_oP_2 = \frac{\mu_0 \chi H_z^{(p)}}{1+\chi N} \qquad (C.1') $$

so that

$$ {}_oP_3 = \frac{\mu_0 \chi H_z^{(p)}}{1+\chi N}\cdot\left\{1+2\cdot\frac{2b^2 a}{3|h|^3}\cdot\frac{\chi}{1+\chi N}\right\} \qquad (C.1'') $$

This produces a new secondary field at the location of 1 and 2 and, therefore, a new polarization of 1 and 2:

$$,P_1 = \frac{\mu_0 \chi H_z^{(p)}}{1+\chi N} + \frac{2b^2 a}{3|h|^3} \cdot P_3 \cdot \frac{\chi}{1+\chi N} = ,P_2 = \qquad (C.2)$$

$$= \frac{\mu_0 \chi H_z^{(p)}}{1+\chi N} \cdot \left\{1 + \frac{2b^2 a}{3|h|^3} \cdot \frac{\chi}{1+\chi N} \cdot \left[1 + 2\,\frac{2b^2 a}{3|h|^3} \cdot \frac{\chi}{1+\chi N}\right]\right\}$$

This in turn produces a new polarization of 3:

$$,P_3 = \frac{\mu_0 \chi H_z^{(p)}}{1+\chi N} + 2\,\frac{2b^2 a}{3|h|^3} \cdot ,P_1 \cdot \frac{\chi}{1+\chi N} =$$

$$= \frac{\chi \mu_0 H_z^{(p)}}{1+\chi N} \cdot \left\{1 + 2 \cdot \frac{2b^2 a}{3|h|^3} \cdot \frac{\chi}{1+\chi N} \cdot \left[1 + \right.\right. \qquad (C.3)$$

$$+ \frac{2b^2 a}{3|h|^3} \cdot \frac{\chi}{1+\chi N} \cdot \left(1 + \right.$$

$$\left.\left. + 2 \cdot \frac{2b^2 a}{3|h|^3} \cdot \frac{\chi}{1+\chi N}\right)\right]\Bigg\}$$

If we call $\frac{2b^2 a}{3|h|^3} \cdot \frac{\chi}{1+\chi N} = u$ (C.3')

one obtains the following scheme:

from Equations (C.2) and (C.2')

$$,P_3 = \frac{\mu_0 \chi H_z^{(p)}}{1+\chi N} \cdot \left\{1 + 2u + 2u^2 + 4u^3\right\} \qquad (C.4)$$

which in turn produces

$$ {}_2P_3 = \frac{\chi \mu_0 H_z^{(p)}}{1+\chi N} + \frac{2b^2 a}{3|h|^3} \cdot {}_1P_3 \cdot \frac{\chi}{1+\chi N} = {}_2P_2 = $$

$$ = \frac{\chi \mu_0 H_z^{(p)}}{1+\chi N} \cdot \{1 + u + 2u^2 + 2u^3 + 4u^4\} \qquad (C.5) $$

which in turn produces a new

$$ {}_2P_3 = \frac{\mu_0 \chi H_z^{(p)}}{1+\chi N} + 2\frac{2b^2 a}{3|h|^3} \cdot {}_2P_1 \cdot \frac{\chi}{1+\chi N} = $$

$$ = \frac{\chi \mu_0 H_z^{(p)}}{1+\chi N} \cdot \{1 + 2u + 2u^2 + 4u^3 + 4u^4 + 8u^5\} \qquad (C.6) $$

which in turn produces a new

$$ {}_3P_1 = \frac{\mu_0 \chi H_z^{(p)}}{1+\chi N} + \frac{2b^2 a}{3|h|^3} \cdot {}_2P_3 \cdot \frac{\chi}{1+\chi N} = {}_3P_2 = $$

$$ = \frac{\mu_0 \chi H_z^{(p)}}{1+\chi N} \cdot \{1 + 2u + 2u^2 + 2u^3 + 4u^4 + 4u^5 + 8u^6\} \qquad (C.7) $$

which in turn produces a new

$$ {}_3P_3 = \frac{\mu_0 \chi H_z^{(p)}}{1+\chi N} + 2\frac{2b^2 a}{3|h|^3} \cdot {}_3P_1 \cdot \frac{\chi}{1+\chi N} = $$

$$ = \frac{\mu_0 \chi H_z^{(p)}}{1+\chi N} \cdot \{1 + 2u + 2u^2 + 4u^3 + 4u^4 + 8u^5 + 8u^6 + 16u^7\} \qquad (C.8) $$

and so on, so that approximately the final magnetic polarization of 3 becomes

$$\infty P_3 = \frac{\mu_0 \chi H_z^{(p)}}{1+\chi N} \cdot \left\{ (1+2u) \cdot \sum_{n=0,1,2}^{\infty} (2u^2)^n \right\} = \frac{\mu_0 \chi H_z^{(p)}}{1+\chi N} \cdot \frac{(1+2u)}{(1-2u^2)} \tag{C.9}$$

and the final magnetic polarization of 1 and 2 becomes:

$$\infty P_1 = \infty P_2 = \frac{\chi \mu_0 H_z^{(p)}}{1+\chi N} \cdot \left\{ (1+u) \cdot \sum_{n=0,1,2}^{\infty} (2u^2)^n \right\} = \frac{\mu_0 \chi H_z^{p}}{1+\chi N} \cdot \frac{(1+u)}{(1-2u^2)} \tag{C.10}$$

and resubstituting Equation (C.3b) and dropping the index ∞ the magnetization of the ellipsoid Nr. 3 in the center is

$$P_3 \doteq \frac{\mu_0 \chi H_z^{(p)}}{1+\chi N} \cdot \frac{1+2 \cdot \frac{2b^2 a}{3|h|^3} \cdot \frac{\chi}{1+\chi N}}{1-2\left(\frac{2b^2 a}{3|h|^3} \cdot \frac{\chi}{1+\chi N}\right)^2} \tag{C.11}$$

and, therefore, the magnetic field inside the center ellipsoid from Equation (C.6) and (C.11):

$$H_3^{(i)} \doteq \frac{H_z^{(p)}}{1+\chi N} \cdot \frac{1+2 \cdot \frac{2b^2 a}{3|h|^3} \cdot \frac{\chi}{1+\chi N}}{1-2\left(\frac{2b^2 a}{3|h|^3} \cdot \frac{\chi}{1+\chi N}\right)^2} \tag{C.12}$$

and the magnetic polarization of the ellipsoids Nr. 1 and 2 at the ends is

$$P_1 = P_2 = \frac{\mu_0 \chi H_z^{(p)}}{1+\chi N} \cdot \frac{1 + \frac{2b^2 a}{3|h|^3} \cdot \frac{\chi}{1+\chi N}}{1 - 2\left(\frac{2b^2 a}{3|h|^3} \cdot \frac{\chi}{1+\chi N}\right)^2} \qquad (C.13)$$

and the magnetic field inside

$$H_1^{(i)} = H_2^{(i)} = \frac{H_z^{(p)}}{1+\chi N} \cdot \frac{1 + \frac{2b^2 a}{3|h|^3} \cdot \frac{\chi}{1+\chi N}}{1 - 2\left(\frac{2b^2 a}{3|h|^3} \cdot \frac{\chi}{1+\chi N}\right)^2} \qquad (C.14)$$

Similarly, as before, the validity of the approximation is constraint by

$$\left(\frac{2b^2 a}{3|h|^3} \frac{\chi}{1+\chi N}\right) \ll 1$$

APPENDIX D - QUANTIFICATION OF PARAMETERS

From Equation (A.29')

$$N = \left(\frac{b}{c}\right)^2 \left[\frac{a}{2c} \ln \frac{a/c+1}{a/c-1} - 1\right]$$

is closely approximated by:

$$N \doteq \left(\frac{a}{c}-1\right)\left(\frac{a}{c}+1\right)\left[\frac{a}{2c} \ln \frac{a/c+1}{a/c-1} - 1\right]$$

for $a/c \to 1$; $\frac{b}{c} \ll 1$

yielding:

$$N \doteq \left(\frac{a}{c} - 1\right) \cdot 2 \left[\frac{1}{2} \ln \frac{2}{a/c-1} - 1\right] =$$

$$\doteq \eta \left[\ln \frac{2}{\eta} - 2\right] \qquad (D.1)$$

where $\eta = \frac{a}{c} - 1 \doteq \frac{1}{2}\left(\frac{b}{a}\right)^2$ and $\frac{a}{c} = \sqrt{1 + \frac{b^2}{c^2}} =$

$$= \frac{a}{\sqrt{a^2-b^2}} \doteq \frac{1}{1-\frac{1}{2}\left(\frac{b}{a}\right)^2} \doteq 1 + \frac{1}{2}\left(\frac{b}{a}\right)^2$$

is used in Table D.1 for $N(b/a)$

Table D.1 - Parameter Values

b/a	η	$2/\eta$	$\ln\frac{2}{\eta}$	$\ln\frac{2}{\eta}-2$	N
1/3	0.06	33.3	3.5	1.5	0.090
1/5	0.02	100.0	4.6	2.6	0.052
1/8	0.0078	256.0	5.54	3.54	0.0275
1/10	0.005	400.0	6.00	4.00	0.0200
1/20	0.00125	1600.0	7.37	5.32	0.0067
1/50	2.10^{-4}	10^4	9.2	7.2	0.00144
1/100	5.10^{-5}	4.10^4	10.58	8.58	$4.29.10^{-4}$
1/15	0.00221	900.0	6.80	4.8	0.0106

Since it is more convenient to work with effective permeabilities, the results of App. A to C are presented in terms of an effective permeability per ferrite ellipsoid as function of intrinsic permeability, geometric dimensions, and location of the ellipsoid in an array.

From the relations $B^{(i)} = \mu_i H^{(i)}$

and $\mu_{eff} = \frac{B^{(i)}}{H^{(p)}}$; $\mu_{rel} = \frac{\mu}{\mu_0}$

Follows from Equation (A.29)

$$\mu_{eff.rel} = \frac{\mu_{i\,rel}}{1+\chi N} = \frac{1+\chi}{1+\chi N} \qquad (D.2)$$

for a single ellipsoid

and from Equation (B.8)

$$\mu_{eff.\,rel} = \frac{1+\chi}{1+\chi N} \cdot \frac{1}{1-\frac{2b^2a}{3|h|^3}\cdot\frac{\chi}{1+\chi N}} \qquad \text{(D.3)}$$

per ellipsoid (i.e., element)

in a two element longitudinal array

From Equation (C.11b) and (C.12):

$$\mu_{\substack{eff.\,rel \\ end}} = \frac{1+\chi}{1+\chi N} \cdot \frac{1+\frac{2b^2a}{3|h|^3}\cdot\frac{\chi}{1+\chi N}}{1-2\left(\frac{2b^2a}{3|h|^3}\cdot\frac{\chi}{1+\chi N}\right)^2} \qquad \text{(D.4)}$$

of the end element

$$\mu_{\substack{eff.\,rel. \\ center}} = \frac{1+\chi}{1+\chi N} \cdot \frac{1+2\cdot\frac{2b^2a}{3|h|^3}\cdot\frac{\chi}{1+\chi N}}{1-2\left(\frac{2b^2a}{3|h|^3}\cdot\frac{\chi}{1+\chi N}\right)^2} \qquad \text{(D.4')}$$

of the center element

in a three element longitudinal array,

(h is the distance from center of one element to the other.)

For large values of the intrinsic permeability $\mu_{i\,rel} > 11$ i.e. $\chi > 10$

the values of $\frac{1+\chi}{1+\chi N}$ are almost the same as of $\frac{\chi}{1+\chi N}$

so that plot 1 H one can be used also for

$$\frac{\chi}{1+\chi} \cdot \frac{1+\chi}{1+\chi N}$$

The term $\frac{2b^2a}{3\mu_1 l^3}$ is normalized with $h = k \cdot 2a$

where k is a multiple of the rod length 2a

$$\frac{2b^2a}{3 \cdot 8 \cdot a^3} \cdot \frac{1}{k^3} = \frac{1}{12}\left(\frac{b}{a}\right)^2 \frac{1}{k^3} = 0.0835 \left(\frac{b}{a}\right)^2 \cdot \frac{1}{k^3}$$

Typical Numerical Values of b/a and $\frac{(ba)^2}{12}$ are given in Table D.2.

Table D.2 - Typical Numerical Values

$\frac{b}{a}$	$\frac{(b/a)^2}{12}$
1/3	0.0093
1/5	0.0034
1/8	0.0013
1/10	0.000835
1/15	0.00037

a. Numerical Examples:

Consider ferrite with an intrinsic $\mu_{i\,rel}$ = 200 at VLF

in form of a rod of length $2a = 16$ cm
and thickness $2b = 2$ cm $\Big\}$ $a/b = 8$

Then from plot 1 follows then

$$\frac{1+K}{1+\chi N} \doteq 30 \qquad \text{and} \qquad \frac{\chi}{1+\chi N} \doteq 30$$

Thus, the relative effective permeability of a single rod is

$$\mu_{eff_{rel}} = 30$$

The effective permeability per rod in a two rod array is given by Equation (D.3) and using Table D.2 with:

$$\mu_{eff_{rel}} = \frac{30}{1 - \frac{0.0013}{k^3} \cdot 30} \doteq 30 \cdot \left[1 + \frac{0.0013}{k^3} \cdot 30 \right]$$

Resultant Numerical values for μeff rel are given in Table D.3.

Table D.3 - Resultant Numerical Values
(2 Elements Longitudinal)

k	μ eff rel	Distance between rod ends Δ = 2a (k-1)
1.13	30 (1 + 0103)	2.08 cm
1.48	30 (1 + 01015)	7.8 cm
1.93	30 (1 + 0.006)	14.9 cm

Hence, in words, Table D.3 expresses the fact, e.g., coupling between the two longitudinally arranged rods amounts to only six per mil, i.e., (0.006) if the ends of the rods are separated by 14.9 cm, about a rod length.

The effective relative permeability per rod in a three rod longitudinal array is with Equation (D.4) and (D.4')

$$\mu_{\substack{eff\,rel \\ end}} = 30 \cdot \frac{1 + \frac{0.0013}{k^3} \cdot 30}{1 - 2 \cdot \left(\frac{0.0013}{k^3} \cdot 30\right)^2}$$

$$\mu_{\substack{eff\,rel \\ center}} = 30 \cdot \frac{1 + 2\,\frac{0.0013}{k^3} \cdot 30}{1 - 2 \cdot \left(\frac{0.0013}{k^3} \cdot 30\right)^2}$$

Resultant Numerical values are given in Table D.4.

Table D.4 - Resultant Numerical Values
(3 Elements Longitudinal)

k	Δ	μ eff rel end	μ eff rel center
1.13	2.08 cm	30 (1 + 0.0318)	30 (1 + 0.0618)
1.48	7.8 cm	30 (1 + 0.01545)	30 (1 + 0.0345)
1.93	14.9 cm	30 (1 + 0.006)	30 (1 + 0.012)

Hence, in words, Table D.4 expresses the fact the mutual coupling between the three rods increases the permeability of the center rod by 3.45% and of the end rods by 1.545% if the distance between rod ends is 7.8 cm, i.e., about one half of the rod length.

(Since the inductance is proportional to the permeability, the percent figures do indicate the mutual inductance relative to the self-inductance of the windings placed on the rods.)

b. Application of Numerical Results to Larger Arrays:

In view of the small coupling between rods one is justified in extending the method to longitudinal arrays with several rods, but using only a first order approach such as represented by formula B.1; i.e., the term n = 0 and n = 1 in Equation (B.7) only. For a six-element array such as shown in Fig. D.1, we can write then immediately:

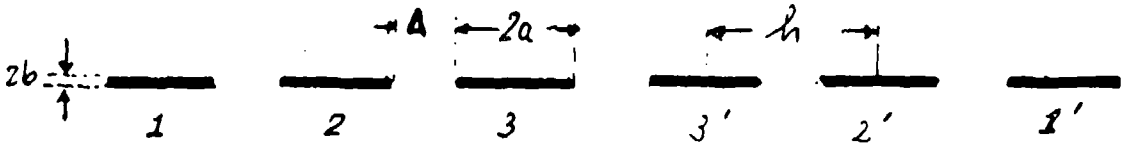

$$\left(\mu_{eff_{rel}}\right)_1 \doteq \frac{1+X}{1+XN}\cdot\left\{1+\frac{X}{1+XN}\cdot\frac{(b/a)^2}{12}\cdot\frac{1}{k^3}\left[\frac{1}{1^3}+\frac{1}{2^3}+\frac{1}{4^3}+\frac{1}{5^3}\right]\right\}$$

$$\left(\mu_{eff_{rel}}\right)_2 \doteq \frac{1+X}{1+XN}\left\{1+\frac{X}{1+XN}\cdot\frac{(b/a)^2}{12}\cdot\frac{1}{k^3}\left[\frac{2}{1^3}+\frac{1}{2^3}+\frac{1}{3^3}+\frac{1}{4^3}\right]\right\}$$

$$\left(\mu_{eff_{rel}}\right)_3 \doteq \frac{1+X}{1+XN}\cdot\left\{1+\frac{X}{1+XN}\cdot\frac{(b/a)^2}{12}\cdot\frac{1}{k^3}\left[\frac{2}{1^3}+\frac{2}{2^3}+\frac{1}{3^3}\right]\right\}$$

Fig. D.1 - Six Element Array

The terms in the curled brackets are:

1.000	2.000	2.000
0.125	0.125	0.250
0.037	0.037	0.037
0.0156	0.0156	2.287
0.000	2.1776	
1.1656		

so that for the same rod material and dimensions as before

$$(\mu_{eff\,rel})_{1\text{ or }1'} \doteq 30 \cdot \left\{1 + 30 \cdot \frac{0.0013}{k^3} \cdot (1.1656)\right\}$$

$$(\mu_{eff\,rel})_{2\text{ or }2'} \doteq 30 \cdot \left\{1 + 30 \cdot \frac{0.0013}{k^3} (2.1776)\right\}$$

$$(\mu_{eff\,rel})_{3\text{ or }3'} \doteq 30 \cdot \left\{1 + 30 \cdot \frac{0.0013}{k^3} \cdot (2.287)\right\}$$

which are evaluated in Table D.5.

Table D.5 - Rel. eff. Permeabilities
(3 Elements Longitudinal)

k	Δ	$(\mu_{eff\,rel})$ 1 or 1'	$(\mu_{eff\,rel})$ 2 or 2'	$(\mu_{eff\,rel})$ 3 or 3'
1.48	7.8 cm	30 (1 + 0.0176)	30 (1 + 0.0325)	30 (1 + 0.0343)
1.93	14.9 cm	30 (1 + 0.007)	30 (1 + 0.0130)	30 (1 + 0.0137)

APPENDIX E - INSERTION OF A SECOND ELLIPSOID OF FERRITE INTO THE COMPOSITE PRIMARY AND SECONDARY FIELD PRODUCED BY THE FIRST ELLIPSOID - TRANSVERSE ARRAY

Fig. E.1 illustrates the situation.

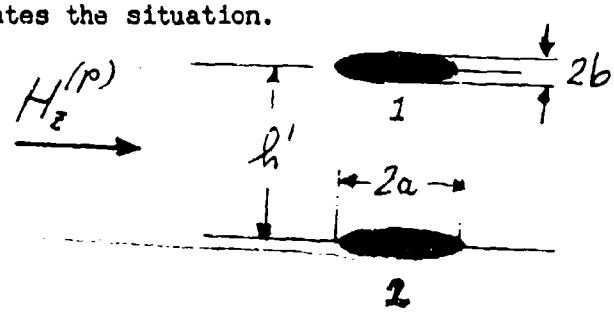

Fig. E.1 - Two Element Transverse Array

(1 and 2 are of the same material and have the same dimensions)

Analogous to Appendix B the second ellipsoid has as its primary field now that described by Equation (A.39') and (A.33') or approximately by (A.34'). This field is not homogeneous anymore. For materials with intrinsically large permeability homogeneous magnetization can be assumed, however, so that the approach is permissible:

$$ {}_0H_2^{(i)} = \frac{H_{II}^{(0)}}{1+\chi N} \tag{E.1} $$

$$ {}_0H_2^{(i)} = \frac{H_2^{(p)}}{1+\chi N}\left[1 - \frac{\chi \frac{b^2 a}{c^3}}{1+\chi N}\left\{\frac{1}{\sqrt{1+(h'/c)^2}} + \frac{1}{2}\ln\frac{\sqrt{1+(h'/c)^2}-1}{\sqrt{1+(h'/c)^2}+1}\right\}\right] \tag{E.1'} $$

For the case $h' \gg a$ the approximation Equation (A.34') can be used

which leads to

$$ {}_0H_2^{(i)} = \frac{H_2^{(p)}}{1+\chi N}\left[1 - \frac{\chi b^2 a}{1+\chi N}\cdot\frac{1}{3(h')^3}\right] \tag{E.2} $$

71 is analogous to 41 except for the sign and the factor 2 of the secondary term. Hence, in full analogy to the development of Equations (B.1) to (B.7), one has now an

$$S = -\frac{b^2 a}{3|h'|^3} \cdot \frac{\chi}{1+\chi N} \qquad (E.2')$$

in the expression for the final

$${}_{\infty}H_2^{(i)} = {}_{\infty}H_1^{(i)} = \frac{H_2^{(p)}}{1+\chi N} \cdot \left\{ \sum_{n=0}^{\infty} (S)^n \right\} \qquad (E.3)$$

yielding for $h' \gg a$ approximately

$$H_2^{(i)} = H_1^{(i)} = \frac{H_2^{(p)}}{1+\chi N} \cdot \frac{1}{1+\frac{b^2 a}{3|h'|^3} \cdot \frac{\chi}{1+\chi N}} \qquad (E.4)$$

and, therefore, the final magnetization

$$P_2 = P_1 = \frac{\mu_0 \chi H_2^{(p)}}{1+\chi N} \cdot \frac{1}{1+\frac{b^2 a}{3|h'|^3} \cdot \frac{\chi}{1+\chi N}} \qquad (E.5)$$

the validity of this approach is constrained by

$$|S| < 1 \quad ; \; h' \gg a$$

If the h' of Figure E.1 is smaller than one half of the rod length a, then the previous approach becomes invalid. The potential of a magnetic dipole follows from Figure 3; and Equation A(A.35)

$$\Psi_D = \frac{Q_m}{4\pi\mu_0}\left[\frac{1}{r_1} - \frac{1}{r_2}\right] \tag{E.6}$$

Applying this formula to the secondary potential field of the first ferrite rod by placing the fictious secondary charges at the focal points of the equivalent ellipsoid yields: $r_1^2 = (z-\kappa)^2+\rho^2$; $r_2^2 = (z+\kappa)^2+\rho^2$

$$\frac{\partial}{\partial z}\Psi^{(s)} = \frac{Q_m}{4\pi\mu_0}\left\{-\frac{1}{2}\frac{2(z-\kappa)}{\left[(z-\kappa)^2+\rho^2\right]^{3/2}} + \frac{1}{2}\frac{2(z+\kappa)}{\left[(z-\kappa)^2+\rho^2\right]^{3/2}}\right\}$$

and the secondary field in the axial direction in a plane z = 0

$$H_z^{(s)} = -\frac{Q_m \cdot 2\kappa}{4\pi\mu_0}\cdot\frac{1}{(\kappa^2+\rho^2)^{3/2}} \tag{E.7}$$

Similarly as the comparison Equation (A.36) and (A.37) the secondary dipole moment can be expressed in terms of the equivalent magnetic polarization (magnetization) yielding

$$2\kappa Q_m = M_m = V_0 \ell \cdot P = \frac{4\pi}{3} b^2 a \cdot P \tag{E.7'}$$

where the initial magnetization is that of the first rod by the primary field:

$${}_0P_1 = \frac{\mu_0 \chi}{1+\chi N}\cdot H^{(p)} \tag{E.7''}$$

so that the axial component of the secondary field of the first rod at the later location of the second rod is with $\rho = h'$

$$H_z^{(s)} = -\frac{\chi}{1+\chi N}\,\frac{b^2 a}{3}\,\frac{H_z^{(p)}}{(\kappa^2+h'^2)^{3/2}} \tag{E.7'''}$$

and the initial total field into which the second rod is inserted is

$$H_{II} = H_z^{(p)} \left\{ 1 - \frac{\chi}{1+\chi N} \cdot \frac{b^2 a/3}{(c^2+h'^2)^{3/2}} \right\} \tag{E.8}$$

which produces a magnetization of the second rod, which in turn via its secondary field changes the magnetization of the first rod and so on, leading to a final magnetization

$$P_1 = P_2 = \frac{\mu_0 \chi H^{(p)}}{1+\chi N} \cdot \sum_{n=0}^{\infty} S^n \tag{E.9}$$

where

$$S' = -\frac{b^2 a}{3[c^2+h'^2]^{3/2}} \cdot \frac{\chi}{1+\chi N} \tag{E.9'}$$

and a corresponding magnetic field inside the rods in the axial direction

$$H_2^{(i)} = H_1^{(i)} = \frac{H_z^{(p)}}{1+\chi N} \cdot \frac{1}{1+\frac{b^2 a}{3[c^2+h'^2]^{3/2}} \cdot \frac{\chi}{1+\chi N}} \tag{E.10}$$

The validity is constrained by $\frac{b^2 a}{3c^3} \cdot \frac{\chi}{1+\chi N} < 1$

Equation (E.10) becomes equal to Equation (E.4) for $h' \gg c$ as expected.

APPENDIX F - INSERTION OF A THIRD ELLIPSOID IN BETWEEN TWO OTHER ELLIPSOIDS, I.E., EXTENSION TO A THREE ELEMENT TRANSVERSE ARRAY

Fig. F.1 illustrates the situation; analogous to Appendix C the initial magnetization of the center ellipsoid Nr. 3 is produced by the primary field and the secondary fields of 1 and 2.

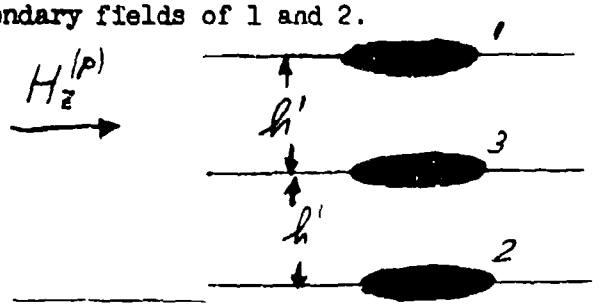

Fig. F.1 - Three Element Transverse Array

In the case $h' \gg a$ with Equation (A.36') and analogous to (C.1)

$$ {}_0P_3 = \frac{\chi}{1+\chi N}\left[\mu_0 H_z^{(p)} - 2\cdot\frac{b^2 a}{3|h'|^3}\cdot {}_0P_1\right] \qquad (F.1) $$

where ${}_0P_1$ is given initially by

$$ {}_0P_1 = {}_0P_2 = \frac{\mu_0 \chi H_z^{(p)}}{1+\chi N} \qquad (F.1') $$

Following the development Equation (C.8) to (C.10) in an analogous fashion with

$$ U = -\frac{b^2 a}{3|h'|^3}\cdot\frac{\chi}{1+\chi N} $$ now instead of that of Equation (C.3')

one obtains the result analogous to Equation (C.11) to (C.14) if one replaces there the term

$$ +\frac{2ba}{3|h'|^3}\cdot\frac{\chi}{1+\chi N} \quad \text{by} \quad -\frac{b^2 a}{3|h'|^3}\cdot\frac{\chi}{1+\chi N} $$

Thus, the magnetic field inside the center ellipsoid is for $h' \gg a$

$$H_3^{(i)} \doteq \frac{H_z^{(p)}}{1+\chi N} \cdot \frac{1 - 2\,\frac{b^2 a}{3|h'|^3} \cdot \frac{\chi}{1+\chi N}}{1 - 2\left(\frac{b^2 a}{3|h'|^3} \cdot \frac{\chi}{1+\chi N}\right)^2} \qquad \text{(F.2)}$$

and the magnetic field inside the outer ellipsoids for $h' \gg a$

$$H_{1\text{ or }2}^{(i)} = \frac{H_z^{p}}{1+\chi N} \cdot \frac{1 - \frac{b^2 a}{3|h'|} \cdot \frac{\chi}{1+\chi N}}{1 - 2\left(\frac{b^2 a}{3|h'|^3} \cdot \frac{\chi}{1+\chi N}\right)^2} \qquad \text{(F.3)}$$

where as before the validity is constraint by $h' \gg a$

$$\frac{b^2 a}{3|h'|^3} \cdot \frac{\chi}{1+\chi N} \ll 1$$

and fully analogous to Appendix E for rod separations $h' \leq c$ one has to replace $|h'|^3$ by $\left[c^2 + h'^2\right]^{3/2}$ in Equation (F.2) and (F.3) giving the magnetic field inside the center ellipsoid approximately

$$H_3^{(i)} = \frac{H_z^{(p)}}{1+\chi N} \cdot \frac{1 - 2\,\frac{b^2 a}{3\left[c^2+h'^2\right]^{3/2}} \cdot \frac{\chi}{1+\chi N}}{1 - 2\left[\frac{b^2 a}{3\left[c^2+h'^2\right]^{3/2}} \cdot \frac{\chi}{1+\chi N}\right]^2} \qquad \text{(F.4)}$$

and the magnetic field inside the outer ellipsoid,

$$H_1 = H_2 = \frac{H_z^{(p)}}{1+\chi N} \cdot \frac{1 - \frac{b^2 a}{3\left[c^2+h'^2\right]^{3/2}} \cdot \frac{\chi}{1+\chi N}}{1 - 2\left[\frac{b^2 a}{3\left[c^2+h'^2\right]^{3/2}} \cdot \frac{\chi}{1+\chi N}\right]^2} \qquad \text{(F.5)}$$

both in the axial direction and

where the validity is constraint by $\frac{b^2 a}{3[c^2+b^{1/2}]^{3/2}} \cdot \frac{K}{1+KN} \ll 1$

APPENDIX G - QUANTIFICATION OF PARAMETERS

Similarly, as in Appendix D, the quantification of parameters for transversal arrays proceeds from the definition of the effective relative permeability per rod. From Equation (E.4) to (E.10) follow the relative effective permeability per rod in a transversal ferrite rod array with two elements:

$$\mu_{eff_{rel}} \doteq \frac{1+\chi}{1+\chi N} \cdot \frac{1}{1+\frac{b^2 a}{3|h'|^3} \cdot \frac{\chi}{1+\chi N}} \qquad (G.1)$$

for a rod separation $|h'| \gg a$

or with approximately

$$\mu_{eff.rel} \doteq \frac{1+\chi}{1+\chi N} \cdot \frac{1}{1+\frac{(b/a)^2}{3\left[1+\left[\frac{h'}{a}\right]^2\right]^{3/2}} \cdot \frac{\chi}{1+\chi N}} \qquad (G.1')$$

for a rod separation h'

$$2b < h' \leq a$$

(In the latter formula, the approximation $c^2 = a^2 - b^2 \doteq a^2$ was used which is permissible for $a/b \geq 3$ i.e., for all practical dimensions of ferrite rods.)

The relative effective permeability per rod in a three element transversal array follows from Equation (F.5) for rod separation $h' \gg a$ with

$$\mu_{\substack{eff.rel \\ center}} \doteq \frac{1+\chi}{1+\chi N} \cdot \frac{1-2\frac{b^2 a}{3|h'|^3} \cdot \frac{\chi}{1+\chi N}}{1-2\left(\frac{b^2 a}{3|h'|^3} \cdot \frac{\chi}{1+\chi N}\right)^2} \qquad (G.2)$$

for the rod in the center of the array

and with

$$\mu_{\substack{eff.rel \\ end}} \doteq \frac{1+\chi}{1+\chi N} \cdot \frac{1-\frac{b^2 a}{3|h'|^3}\cdot\frac{\chi}{1+\chi N}}{1-2\left(\frac{b^2 a}{3|h'|^3}\cdot\frac{\chi}{1+\chi N}\right)^2} \qquad (G.2')$$

for a rod at the end of the array.

For rod separations $2b < h' < a$ the respective relative effective permeabilities are approximately from Equation (F.4) and (F.5):

$$\mu_{\substack{eff.rel \\ center}} = \frac{1+\chi}{1+\chi N} \cdot \frac{1-2\frac{\chi(b/a)^2}{1+\chi N}\cdot\frac{1}{3\left[1+(h'/a)^2\right]^{3/2}}}{1-2\left[\frac{\chi(b/a)^2}{1+\chi N}\cdot\frac{1}{3\left[1+(h'/a)^2\right]^{3/2}}\right]^2} \qquad (G.3).$$

$$\mu_{\substack{eff.rel \\ end}} = \frac{1+\chi}{1+\chi N} \cdot \frac{1-\frac{\chi(b/a)^2}{1+\chi N}\cdot\frac{1}{3\left[1+(h'/a)^2\right]^{3/2}}}{1-2\left[\frac{\chi(b/a)^2}{1+\chi N}\cdot\frac{1}{3\left[1+(h'/a)^2\right]^{3/2}}\right]^2} \qquad (G.3')$$

Similarly, as in Appendix D, the rod separation h' will be used in normalized form:

$$h' = k' \cdot 2b$$

i.e., h; is measured in multiples of the rod diameter. Introduction of this normalization into Equation (G.1) to (G.3') gives:

For the two element transversal array from Equation (G.1)

$$\mu_{eff.rel} \doteq \frac{1+X}{1+XN} \cdot \frac{1}{1+\frac{a/b}{24}\cdot\frac{X}{1+XN}\cdot\frac{1}{|k'|^3}}$$

for values of

$$k' \gg \frac{a}{2b} > 1$$

from Equation (G.1')

$$\mu_{eff.rel} = \frac{1+X}{1+XN} \cdot \frac{1}{1+\frac{(b/a)^2 X}{1+XN}\cdot\frac{1}{3\left[1+(b/a)^2(2k')^2\right]^{3/2}}}$$

for values of

$$1 < k' \leq \frac{a}{2b}$$

and for the three element transversal array from Equation (G.2) and (G.3)

$$\mu_{eff.rel\ center} = \frac{1+X}{1+XN} \cdot \frac{1-2\cdot\frac{a/b}{24}\cdot\frac{X}{1+XN}\cdot\frac{1}{|k'|^3}}{1-2\left(\frac{a/b}{24}\cdot\frac{X}{1+XN}\cdot\frac{1}{|k'|^3}\right)^2}$$

$$\mu_{eff.rel\ end} \doteq \frac{1+X}{1+XN} \cdot \frac{1-\frac{a/b}{24}\cdot\frac{X}{1+XN}\cdot\frac{1}{|k'|^3}}{1-2\left(\frac{a/b}{24}\cdot\frac{X}{1+XN}\cdot\frac{1}{|k'|^3}\right)^2}$$

for $k' \gg \frac{a}{2b} > 1$

or from Equation (G.2') and (G.3')

$$\mu_{eff.rel.\ center} \doteq \frac{1+\chi}{1+\chi N} \cdot \frac{1 - 2\,\frac{\chi (b/a)^2}{1+\chi N} \cdot \frac{1}{3\left[1+(b/a)^2(2k')^2\right]^{3/2}}}{\left[1 - 2\,\frac{\chi (b/a)^2}{1+\chi N} \cdot \frac{1}{3\left[1+(b/a)^2(2k')^2\right]^{3/2}}\right]^2}$$

$$\mu_{eff.rel\ end} \simeq \frac{1+\chi}{1+\chi N} \cdot \frac{1 - \frac{\chi (b/a)^2}{1+\chi N} \cdot \frac{1}{3\left[1+(b/a)^2(2k')^2\right]^{3/2}}}{\left[1 - 2\,\frac{\chi (b/a)^2}{1+\chi N} \cdot \frac{1}{3\left[1+(b/a)^2(2k')^2\right]^{3/2}}\right]^2}$$

for $1 < k' \leq a/b$

a. Numerical Evaluation of the Equations (G.1) and (G.1'):

Two rod transversal array:

Consider as before in Appendix D a practical value

and $$\frac{\chi}{1+\chi N} \approx \frac{1+\chi}{1+\chi N} \doteq 30$$

and writing for the two element array the effective relative permeability as:

$$\mu_{eff\,rel} \doteq 30\ \frac{1}{1+\Delta} \doteq 30(1-\Delta)$$

where $\Delta \ll 1$

the relative deviation from the single rod effective relative permeability. Table G.1 is obtained for the effective relative permeability per rod in a two element transversal array as a function of rod separation, in multiples k' of rod diameters 2b.

Table G.1 - Effective Relative Permeabilities of Rods in an Array (2 Element Transverse)

$k' = \frac{h'}{2b}$	μ rel eff per rod	Δ %
1	30 (1 - 0.142)	-14
1.5	30 (1 - 0.13)	-13
2.0	30 (1 - 0.112)	-11
2.5	30 (1 - 0.096)	-10
3.0	30 (1 - 0.08)	- 8
4.0	30 (1 - 0.056)	- 5.6
6.0	30 (1 - 0.0266)	- 2.6
8.0	30 (1 - 0.014)	- 1.4
10.0	30 (1 - 0.008)	- 0.8
20.0	30 (1 - 0.00125)	- 0.125
∞	30	0

b. Numerical Evaluation of Equations (2.2) through (3.3):

Three rod transversal array:

Like in a. before, consider $a/b = 8 \quad \chi = 199$

Because of the negligible influence of $2\Delta^2$ in the denominator of the formulas, Table G.1 can be used readily for their evaluation, leading to Table G.2 the permeability of center and end rod in a three rod transversal array as function of rod separation in multiplex of rod diameters.

Table G.2 - Effective Relative Permeabilities of Rods in an Array
(3 Element Transverse)

$k' = \frac{h'}{2b}$	μ end rod rel eff	μ center rod rel eff
1	30 (1 - 0.14)	30 (1 - 0.28)
1.5	30 (1 - 0.13)	30 (1 - 0.26)
2.0	30 (1 - 0.11)	30 (1 - 0.22)
2.5	30 (1 - 0.096)	30 (1 - 0.192)
3.0	30 (1 - 0.08)	30 (1 - 0.16)
4.0	30 (1 - 0.056)	30 (1 - 0.11)
6.0	30 (1 - 0.0266)	30 (1 - 0.052)
8.0	30 (1 - 0.014)	30 (1 - 0.028)
10	30 (1 - 0.008)	30 (1 - 0.016)
20	30 (1 - 0.00125)	30 (1 - 0.0025)
∞	30	30